Title
CHARACTERIZATION OF SINTERING PHENOMENA OF (Na^K) ?=) NbO

Author
Stannek, Wolfgang.

Publication Date
1970-07-01

UCRL-19668

c.2

CHARACTERIZATION OF SINTERING PHENOMENA OF $(Na_{0.5}K_{0.5})NbO_3$

Wolfgang Stannek
(M.S. Thesis)

July 1970

AEC Contract No. W-7405-eng-48

LAWRENCE RADIATION LABORATORY
UNIVERSITY of CALIFORNIA BERKELEY

UCRL-19668 c.2

DISCLAIMER

CHARACTERIZATION OF SINTERING PHENOMENA OF $(Na_{0.5}K_{0.5})NbO_3$

Contents

CHARACTERIZATION OF SINTERING PHENOMENA OF $(Na_{0.5}K_{0.5})NbO_3$

Wolfgang Stannek

Inorganic Materials Research Division, Lawrence Radiation Laboratory,
and Department of Materials Science and Engineering,
College of Engineering, University of California
Berkeley, California

July 1970

ABSTRACT

Investigations of sintering behavior, densification and grain growth of pure and barium-doped sodium-potassium niobate of the composition $(Na_{0.5}K_{0.5})NbO_3$ were made in an oxygen atmosphere at several temperatures. Calcining conditions were optimized in preceding experiments. X-ray diffraction, microprobe analysis, weight loss data, scanning electron microscope and sintering data were used to characterize this compound. A decrease in density accompanied by large grain growth and an increase in pore size was observed. Examinations employing a scanning electron microscope revealed a microstructure consisting of well marked cubical grains. Ba^{2+} doped into the material in several amounts appeared to be a powerful grain growth inhibitor in this system. It is postulated that the low surface energy at the (100) planes of sodium-potassium niobates is responsible for the difficulties in conventional processing of these materials.

I. INTRODUCTION

Compounds of the perovskite-type structure, especially the titanates and niobates, have received considerable interest in recent years because of their ferroelectric properties. The solid solution system between $NaNbO_3$ and $KNbO_3$ is reported to have low dielectric constants and high electromechanical coupling coefficients.[1] Such properties are desirable for certain ultrasonic delay-line applications requiring thin-section transducers.[2] Earlier work by Shirane et al.[3] has shown that most of the phases in this system are ferroelectric at room temperature except those very close to the $NaNbO_3$ side of the diagram. Sodium-potassium niobate of the composition $(Na_{0.5}K_{0.5})NbO_3$ is reported to possess the most desirable ferroelectric properties.[4,5]

Conventional processing of sodium-potassium niobates results in poor structures of the fired bodies; in particular, a residual porosity undesirable for thin-section applications was reported by L. Egerton et al.[6] Furthermore, difficulties seem to exist in sintering these materials to sufficiently homogeneous dense ceramics possessing an adequate fine grained microstructure. As a result of these problems, most of the ceramic work done in the sodium-potassium niobate system is carried out using hot-pressing techniques and little is reported about sintering. Although capable of supplying quality material, hot-pressing is not a technique to provide a high volume low cost material.

The purpose of this study was to investigate and to describe the compound $(Na_{0.5}K_{0.5})NbO_3$, to characterize its behavior in conventional processing, and to determine, and if possible to eliminate, the factors which are constantly leading to poor results in the sintered bodies.

A. Potassium Niobate $KNbO_3$

Potassium niobate has the ideal perovskite structure above its Curie temperature of 435°C.[3] On cooling, the material undergoes the following two phase transitions which are connected with detectable temperature hysteresis:

$KNbO_3$: Orthorhombic $\overset{225°C}{\longleftrightarrow}$ tetragonal $\overset{435°C}{\longleftrightarrow}$ cubic

These phase transitions are quite similar to those of $BaTiO_3$.

The phase diagram of the system K_2O-K_2CO_3 and Nb_2O_5 as shown in Fig. 1 has been investigated by Reisman and Holtzberg.[7] It can be seen from the diagram that there are five well-defined compounds. The compound $KNbO_3$ corresponding to the composition 50 mole % K_2O and 50 mole % Nb_2O_5 melts incongruently at a temperature of 1039°C. $KNbO_3$ is reported to possess a marked tendency to lose oxygen, especially in the vicinity of the peritectic. Weight losses of the order of 0.1% accompanied with reduction exhibited a dark blue to black coloration of the material.

The lattice parameters of orthorhombic $KNbO_3$ at room temperature are reported to be:[1]

$$a' = c' = 4.037\ \text{Å}$$

$$b = 3.9711\ \text{Å}$$

$$\beta = 90°\ 15'$$

The orthorhombic distortion is described in terms of monoclinic axes. $KNbO_3$ is not known to form a multiple unit cell.

B. Sodium Niobate $NaNbO_3$

The dielectric and crystallographic properties of $NaNbO_3$ are quite complex in sharp contrast with the well-defined situation encountered in $KNbO_3$. The question whether or not $NaNbO_3$ is ferroelectric was rather

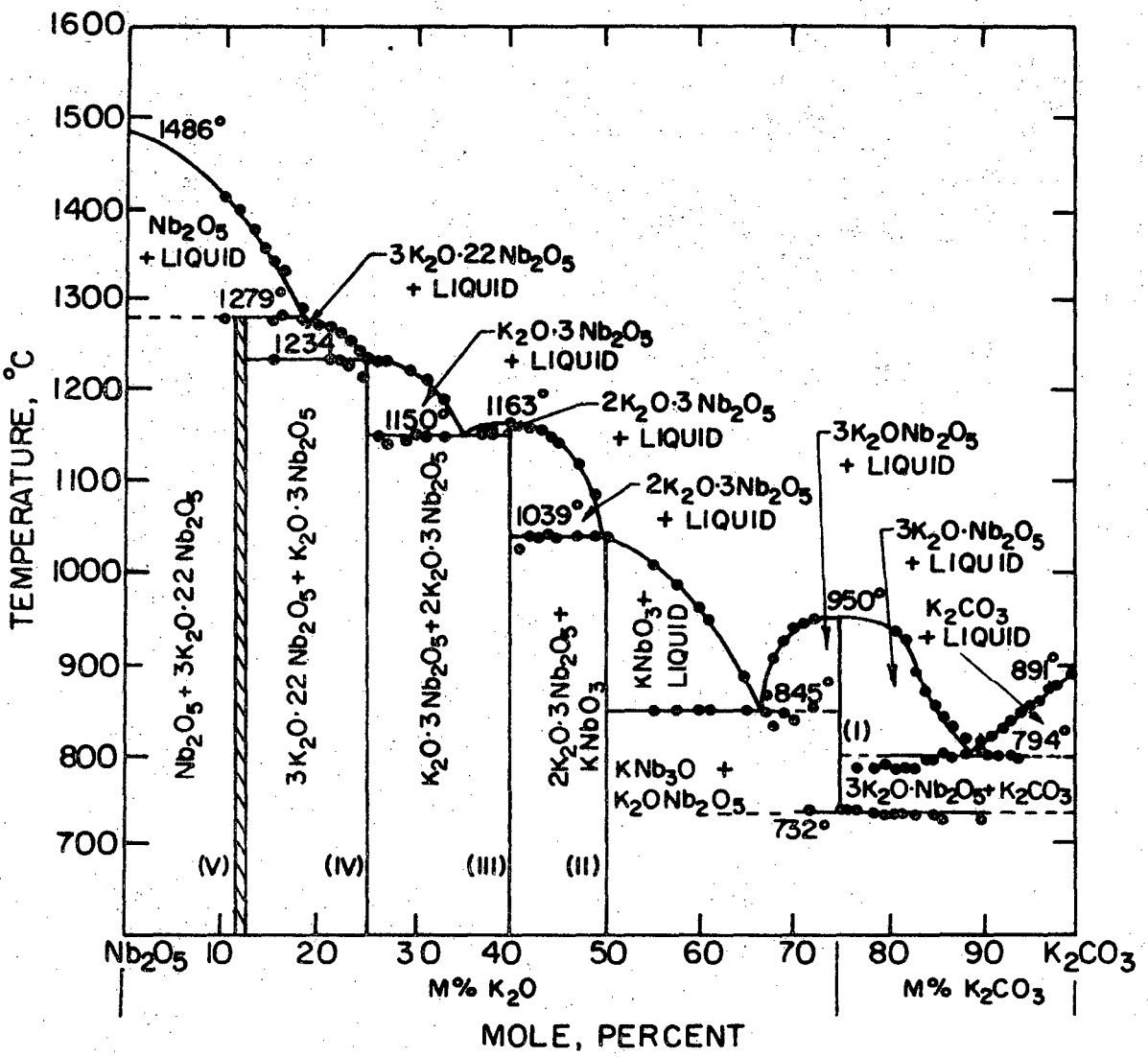

XBL 707-1464

Fig. 1. Phase diagram of the system K_2O-K_2CO_3-Nb_2O_5 (Ref. 7).

confusing until recent careful studies of the dielectric properties showed that $NaNbO_3$ at room temperature is truly antiferroelectric. However, a ferroelectric state can be induced by the application of strong fields.

The phase transition occurring in $NaNbO_3$ have been studied by a number of authors. Reisman et al. reported the transition between the tetragonal and cubic phase at a temperature of 480°C. The phase diagram as shown in Fig. 2 was investigated by Shafer and Roy.[8] Consequently, $NaNbO_3$ exhibits the following phase transitions:

$NaNbO_3$: Orthorhombic $\overset{368°C}{\longleftrightarrow}$ tetragonal $\overset{640°C}{\longleftrightarrow}$ cubic

Later on in a correction of the inaccuracy in the earlier paper, Reisman et al.[9] were able to show that the transition temperature between tetragonal and cubic phase is very sensitive to the state of strain in the samples.

The compound $NaNbO_3$ corresponding to the composition 50 mole % Na_2O and 50 mole % Nb_2O_5 melts congruently at a temperature of 1412°C. The liquid is reported to be very fluid.

The lattice parameters of orthorhombic $NaNbO_3$ at room temperature are reported to be:

$$a' = c' = 3.915\ \text{Å}$$

$$b = 3.88\ \text{Å}$$

$$\beta = 90°\ 41'$$

The orthorhombic distortion is described in terms of monoclinic axes. $NaNbO_3$ is known to form a multiple unit cell.

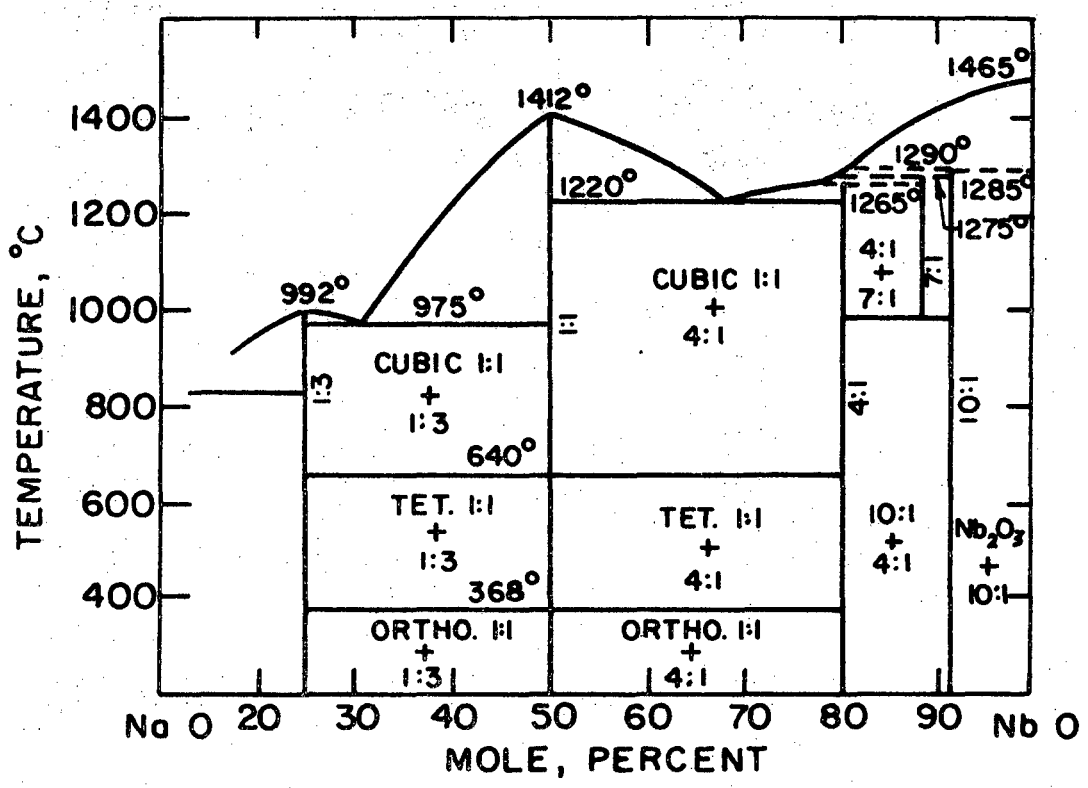

XBL 707-1465

Fig. 2. Phase diagram of the system Na_2O-Nb_2O_5 (Ref. 8).

C. Solid Solutions of $KNbO_3$ and $NaNbO_3$

Despite of the large difference between the ionic radii of sodium and potassium, the two niobates form a solid solution across the whole composition range.[3] No miscibility gap was found to exist between the pure $NaNbO_3$ and the pure $KNbO_3$ orthorhombic structures. This fact is supported by the continuous change in lattice constants[3] and in density over the whole range of compositions. The appearance of the wide solid solution range becomes more understandable, however, if one discusses the interaction of the cations with the anionic entity present in terms of some potential. In this respect, the cation-oxygen attraction, expressed as either field strength or ionic potential (cation charge/cation radius), has proved a useful parameter for assessing the relative power of a cation to satisfy its coordination requirements and to dictate the configuration.[10] Table I contains the ionic radii and the ionic potentials (Z/r) of all ions present.

Table I. Radius and ionic potential of ions

Ion	Radius in Å	Ionic potential (Z/r)
Nb^{5+}	0.69	7.25
Na^{1+}	0.94	1.07
K^{1+}	1.33	0.75
Ba^{2+}	1.34	1.50
O^{2-}	1.40	

It is shown in the table that Nb^{5+} dictates the spacial arrangement of oxygen; no other cation present could successfully compete with

niobium (5+). Thus, the structures of the solid solutions are determined by the very stable NbO_6-octahedra which will be more or less distorted depending upon which of the cations is occupying the A-site of the $A^{1+}B^{5+}O_3$ structure. Therefore, it is not unusual to see that despite of the large differences between the ionic radii and the polarizabilities of sodium and potassium, the Curie temperature remains almost constant over the whole system of solid solutions, except, of course, for the region near $NaNbO_3$.

No great change with respect to the crystallographic factors was expected by introducing Ba^{2+} in several amounts into $(Na_{0.5}K_{0.5})NbO_3$. Such a substitution of barium ions for sodium and/or potassium creates cation vacancies in the A-sites of the lattice. The theoretical formula of a sodium-potassium niobate doped with 1 at % Ba^{2+} can be written as:

$(Na_{0.49}K_{0.49})Ba_{0.01}\square_{0.01}NbO_3$

$\square$ = cation vacancies

The Ba^{2+} doped into the batches was expected to increase the diffusivity of Nb^{5+} which was thought to be the rate determining species in sintering. A consideration of the structure of sodium-potassium niobate shows NbO_6-octahedra which are sharing corners. In order to diffuse through the lattice Nb^{5+} has to jump in a first step from its 6-fold octahedral site to a vacant A-site having a 12-fold coordination. In a second jump Nb^{5+} can occupy a new octahedral site.

The theoretical density of undoped sodium-potassium niobate of the composition $(Na_{0.5}K_{0.5})NbO_3$ is reported to be 4.51 gr/cm^3. The lattice parameters versus composition of the whole solid solution range between the end members $NaNbO_3$ and $KNbO_3$ have been determined by Shirane et al.[3]

II. EXPERIMENTAL PROCEDURE AND RESULTS

A. Preparation of Sodium-Potassium Niobate Powder

1. Starting Materials

Batches used in the first experiments were prepared by mixing Nb_2O_5, Na_2CO_3, K_2CO_3 and $BaCO_3$ as starting materials. Table II gives the analysis of the carbonates as supplied by the manufacturers. Table III shows the results of a semi-quantitative spectrographic analysis on Nb_2O_5 (99.5%) and $BaCO_3$ (99.0%) carried out by the American Spectrographic Laboratories, Inc.

Table II. Chemical analysis on the carbonates as given by the producers

	Na_2CO_3 Baker's reagent grade 99.8 wt %	K_2CO_3 Mallinckrodt's reagent grade 99.8 wt %	$BaCO_3$ Baker's reagent grade 99.0 wt %
NH_4OH	0.003	0.01	
As	0.00004	0.0001	
Cu + Mg	0.004	0.01	0.05
Cl	0.0008	0.003	0.002
Heavy metals	0.0002	0.0005	0.001
Fe	0.0002	0.0005	0.001
N	0.0005	0.001	0.005
PO_4^{---}	0.0003	0.001	
SiO_2	0.0002	0.005	
Na	-	0.02	
SO_4^{--}	0.001	0.004	
K	0.004	-	

Table III. Results of a semi-quantitative spectrographic analysis* on Nb_2O_5 and $BaCO_3$

	Nb_2O_5 Alfa Inorganic 99.5 wt %	$BaCO_3$ Baker's reagent grade 99.0 wt %
Ba**	<0.001	-
Mg	-	0.002
Al	0.08	<0.003
Si	0.01	<0.01
Ca	0.015	0.005
V	0.005	-
Fe	-	-
Cu	<0.02	0.0005
Sr	-	0.08

* Reported by American Spectrographic Laboratories, Inc.

** All reported as oxides in wt %.

Because of its very large particle size and the broad particle size distribution range, the Nb_2O_5 powder was dry ground for 50 hrs using a "Sweco" multiple chamber vibration mill. A polyurethane lined container was chosen for this milling process using Lucite balls as grinding media in order to avoid an increase of impurities due to abrasian which are difficult to remove.

After grinding, the Nb_2O_5 powder was screened through a 115 mesh sieve. The screened powder was poured into a glass jar covered with aluminum foil and placed in a "Hevi Duty" furnace. The furnace was

slowly brougnt to a temperature of 450°C establishing a heating rate of 3-4 degrees per minute. After reaching this temperature, the Nb_2O_5 powder was held for 24 hrs in order to burn out the plastic material introduced during the grinding process. Earlier experiments determining soaking time and temperature for decomposition of Lucite have shown a temperature of 450°C and a soaking time of 24 hrs to be sufficient to obtain constant weight of the ground material. Final measurements of particle size using a "Fisher's Sub Sieve Sizer" revealed an average particle size of 1.30 μm. Measurements using the scanning electron microscope showed a particle size distribution from 0.3 to 1.5 μm. Figure 3 taken with the scanning electron microscope shows a representative portion of the Nb_2O_5 powder as processed. The shape of the particles is quite irregular. In general, the grains are somewhat rounded off, sometimes approaching a spherical shape rather than cubical.

The Nb_2O_5 powder as processed was kept in a dessicator until usage.

A further processing of the other raw materials Na_2CO_3, K_2CO_3 and $BaCO_3$ was not necessary because the particle size of these materials was sufficiently small.

2. Powder Preparation with Carbonates as Starting Materials

A standard technique was developed and employed for preparation of all powder samples made out of carbonates as starting materials.

After drying the raw materials at 105°C in an electric oven for 50 hrs, the reagent grade Na_2CO_3 and K_2CO_3, together with Nb_2O_5, were weighed in proper portions to give a 3 mole batch of powder of the composition $(Na_{0.5}K_{0.5})NbO_3$.

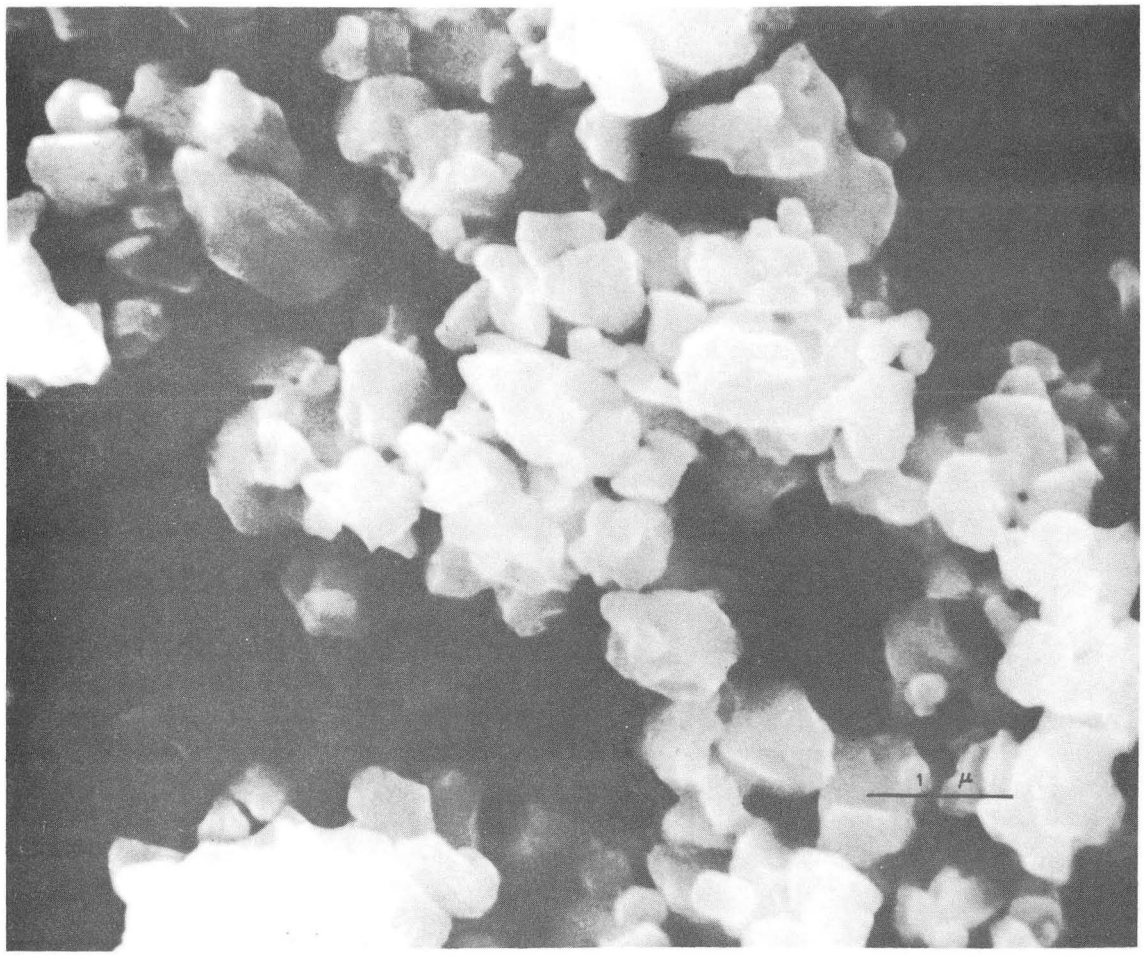

XBB 707-3222

Fig. 3. Scanning electron micrograph of Nb_2O_5 powder after processing.

The raw materials were placed in a rubber lined ball mill using teflon balls as grinding and mixing media. To minimize contaminations during mixing, 1000 ml of isopropyl alcohol was added to about 600 gr of dry raw material. The ball mill, having a diameter of 16 cm, was allowed to tumble at 40 rpm for 50 hrs. The mixing time of 50 hrs determined in earlier experiments was found to give sufficiently homogeneous materials.

After the mixing process, the contents of the ball mill were poured into a glass beaker which was put on an electric hot plate having a magnetic stirrer. The mixture, consisting of the raw materials and isopropyl alcohol, was heated to a temperature of about 90°C which is sufficiently high to evaporate isopropyl alcohol. Immediately after pouring the mixture into the glass beaker, the magnetic stirrer was turned on. Stirring was continued through the whole evaporation process in order to prevent segregations of the heavier constituents of the batch. At the point where stirrer could not move, the beaker was placed in an electric oven for 24 hrs at a temperature of 105°C. This final drying step was followed by a dry milling process for 50 hrs in a "Sweco" vibration mill using a polyurethane lined container with teflon balls as grinding media. After finishing the mixing process, the powder was filled into polyethylene bottles which were kept closed in a dessicator.

At this state, initial calcining experiments were made. Small amounts of powder were calcined in a platinum crucible at an arbitrarily chosen temperature of 900°C for 6 hrs. The high temperature and the long calcining time were chosen in order to obtain good reaction of the powder. X-ray powder diffraction patterns were made on -115 mesh portions of the calcined material. The evaluation of these patterns revealed,

besides the main peaks of $(Na_{0.5}K_{0.5})NbO_3$, smaller peaks due to $Na_2Nb_8O_{21}$ and $K_2Nb_8O_{21}$. Calculations for correction were carried out on the basis of the intensity of the extra peaks. Further experiments showed an excess of 1.5 mole % Na_2CO_3 and 1.5 mole % K_2CO_3 to be just sufficient to eliminate the extra lines. Figure 4 shows X-ray powder diffraction patterns on materials with and without excess carbonates. All further batches prepared with carbonates had the same amount of excess $Na2CO_3$ and K_2CO_3. The stoichiometry of every batch was checked by means of X-ray powder patterns.

This standard technique for preparing powders using carbonates as starting materials was employed to produce sodium-potassium niobate powders pure and doped with several amounts of $BaCO_3$. Powder samples having the following theoretical compositions were prepared:

$(Na_{0.495}K_{0.495})Ba_{0.005}\square_{0.005}NbO_3$

$(Na_{0.490}K_{0.490})Ba_{0.01}\square_{0.01}NbO_3$

$(Na_{0.48}K_{0.48})Ba_{0.02}\square_{0.02}NbO_3$

$(Na_{0.46}K_{0.46})Ba_{0.04}\square_{0.04}NbO_3$

3. Powder Preparation with Nitrates as Starting Materials

Nitrates as starting materials were chosen for two important reasons:

(1) Because of their low decomposition temperatures, see Table IV;

(2) Because of their very good solubility in hot and cold water, see Table IV.

The following chemicals were chosen for preparation of powder samples using nitrates as starting materials, $NaNO_3$ 99.9%, KNO_3 99.1%,

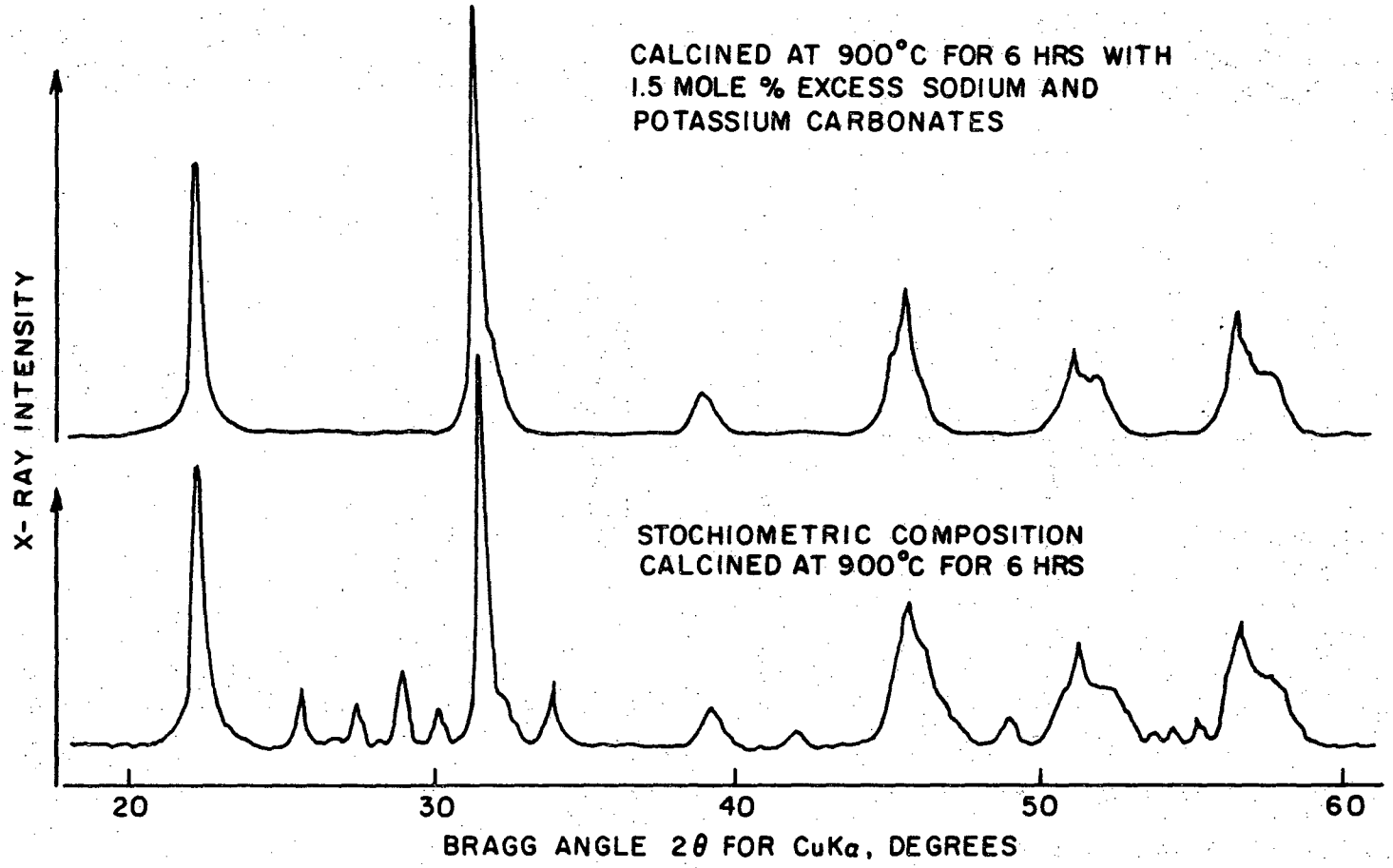

XBL 707-1466

Fig. 4. Comparison of X-ray diffraction powder patterns of $(Na_{0.5}K_{0.5})NbO_3$ calcined with and without excess sodium and potassium carbonates.

Table IV. Decomposition temperatures and solubilities of sodium, potassium and barium nitrate

	Decomposition temperature in °C	Solubility in H_2O 25°C g/100 ml	Solubility in H_2O 100°C g/100 ml
$NaNO_3$	380	73	180
KNO_3	400	13.3	247
$Ba(NO_3)_2$	592	8.7	34.2

and $Ba(NO_3)_2$ 99.5%. The same processed Nb_2O_5 powder was used as described under II-A-1.

Table V shows the impurities of the nitrates used as raw materials as given by the producer.

After drying the nitrates in an electric oven for 50 hrs at a temperature of 105°C, the reagent grade $NaNO_3$, KNO_3, and $Ba(NO_3)_2$, together with Nb_2O_5 powder, were weighed in proper portions to give 0.5 mole batches of each of the following three compositions:

$(Na_{0.495}K_{0.495})Ba_{0.005}\square_{0.005}NbO_3$

$(Na_{0.49}K_{0.49})Ba_{0.01}\square_{0.01}NbO_3$

$(Na_{0.46}K_{0.46})Ba_{0.04}\square_{0.04}NbO_3$

Each of the batches was poured into a glass beaker; 500 ml of distilled and degased water were added. The beakers were placed on an electric hot plate having a magnetic stirrer. Before inspissating, the solution was kept at a temperature of about 90°C and stirred for 2 hrs. Then the temperature was raised so that the solution started boiling.

Table V. Chemical analysis of the nitrates as given by the producer*

	$NaNO_3$ 99.9 wt %	KNO_3 99.1 wt %	$Ba(NO_3)_2$ 99.5 wt %
Cl	0.001	0.002	0.0003
IO_3	<0.0005	<0.0005	
NO_3	<0.001	<0.001	
PO_4^{---}	0.0002	0.00005	
SO_4^{--}	0.001	0.0005	0.025
R_2O_3	0.002	0.0005	
Pb	0.0002	0.0002	0.0005
Fe	0.0001	0.00005	0.0001
K	0.004	-	
Na	-	0.004	
Ca, Sr	-	-	0.035

* J. T. Baker Chemical Co., Phillipsburg, N.J.

At the point the stirrer stopped due to the high viscosity, the beaker was put into an electric oven for 24 hrs at a temperature of 110°C. After this final drying process, the cake consisting of mixed raw materials was crushed slightly and filled into polyethylene bottles which were kept in a dessicator.

Small portions of powder prepared with nitrates as starting materials were calcined for 6 hrs at a temperature of 900°C. Their stoichiometry was also checked by means of powder X-ray diffraction methods. The same

extra peaks due to $Na_2Nb_8O_{21}$ and $K_2Nb_8O_{21}$ were present but having a somewhat weaker intensity. The elimination of these peaks could be achieved by adding 1.3 mole % $NaNO_3$ and 1.3 mole % KNO_3.

B. Calcination of the Mixed Raw Materials

An attempt to find some useful data in the literature regarding calcining time and temperature failed because of the very wide spread of values reported.[1,6] Calcining temperatures ranged from 750 to 1000°C and calcining times from 1 to 20 hrs. Therefore, experiments were carried out to determine and optimize both the calcining time and temperature using the density obtained in a standard sintering treatment as a guide.

1. Optimization of Calcining Temperature

Experiments were carried out using powder of the composition $(Na_{0.5}K_{0.5})NbO_3$ prepared with carbonates. About 170 gr of this powder was filled into a "Visten" plastic tubing which was closed and sealed at both ends and inserted into an isostatic press. The isostatic pressing of the dry powder at room temperature produced a green body of relatively high and uniform density which facilitated handling. A pressure of 30,000 psi applied for 10 min was suitable for pressing this powder. The preformed slug was cut by means of a band saw into eight slices of about equal weight. This series of slices was calcined in air for 2 hrs in a platinum crucible. The calcining temperature was varied between 550 and 900°C in 50° degree intervals.

X-ray diffraction powder patterns were made of each of the calcined specimens to check the degree of reaction at a specific temperature. Figures 5 and 6 show four of the patterns obtained.

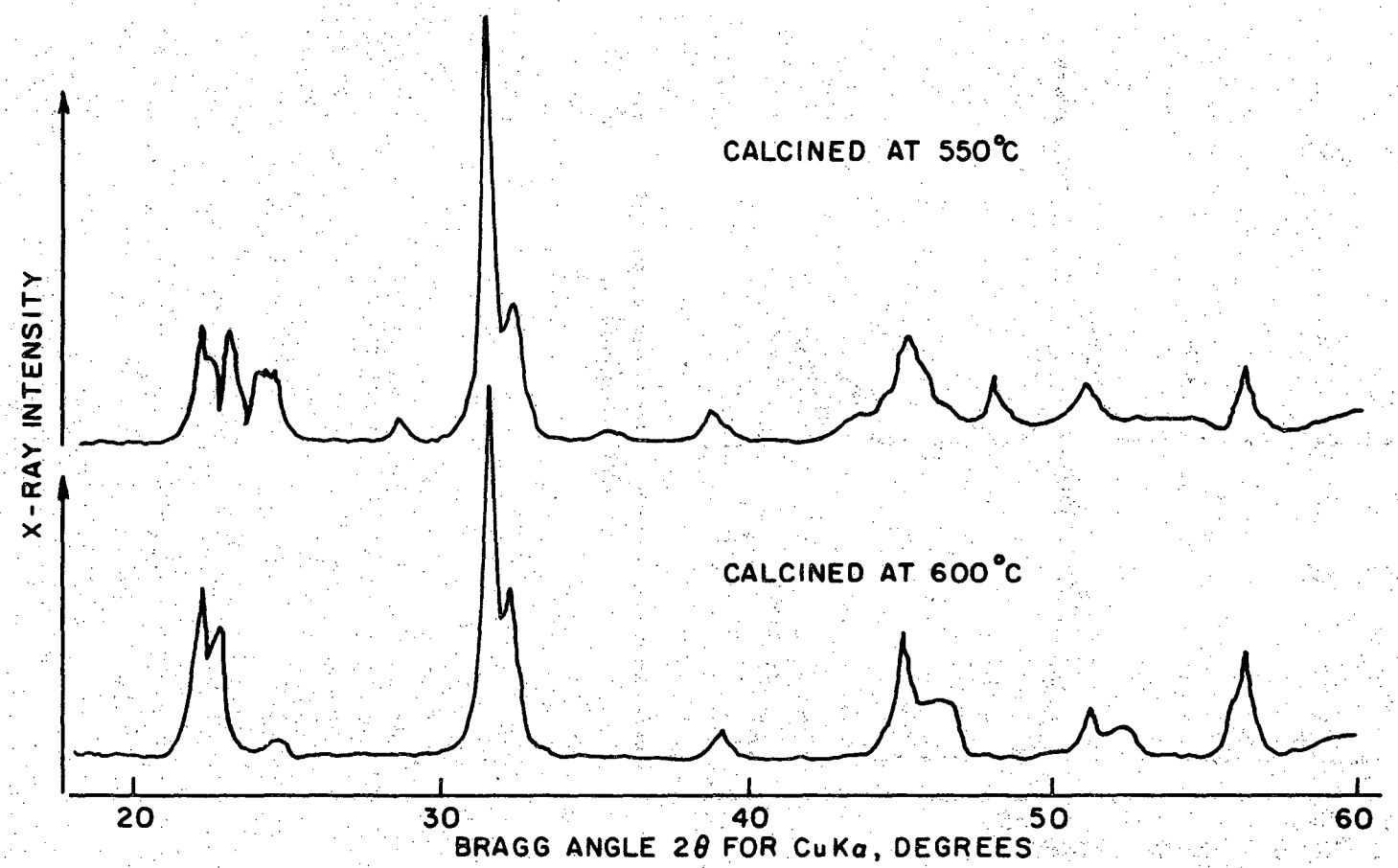

XBL 707-1467

Fig. 5. Comparison of X-ray diffraction powder patterns of samples calcined at 550°C and 600°C for 2 hrs.

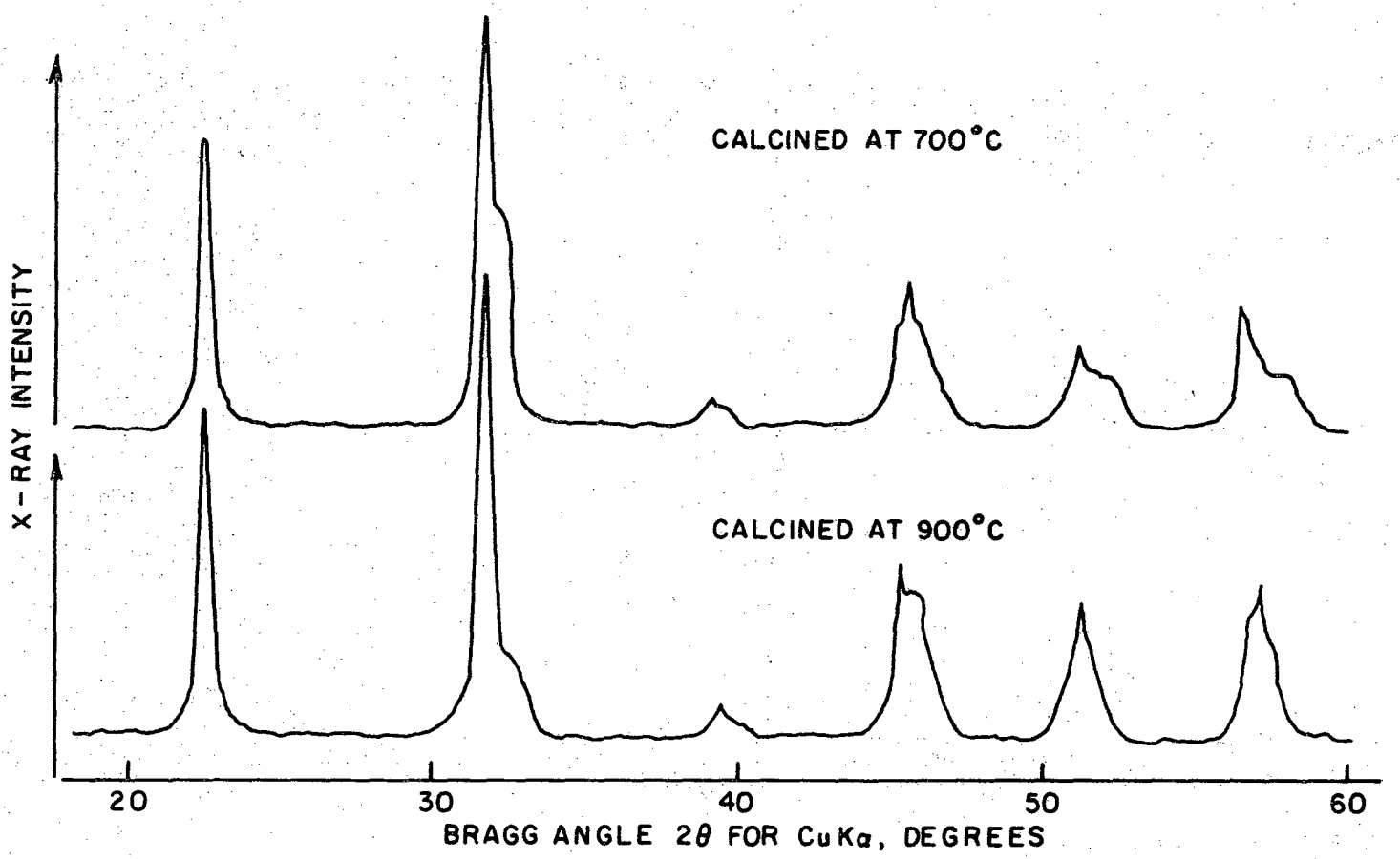

XBL 707-1468

Fig. 6. Comparison of X-ray diffraction powder patterns of samples calcined at 700°C and 900°C for 2 hrs.

Pellets 3/4 inch in diameter and about 1/8 inch thick were pressed of each calcined powder sample using a tungsten alloy steel die. These pellets were packed into a platinum crucible separated by layers of calcined packing powder of the same composition and sintered in air at a temperature of 1050°C for 2 hrs. After cooling, both diameter of the pellets and their density were measured. These results are shown in Figs. 7 and 8.

2. Optimization of Calcining Time

The experiments to determine the optimum time of calcining were carried out with powder taken from the same batch as for optimization of calcining temperature. The sample preparation was basically the same as described already under point 1.

The isostatically pressed slug of uncalcined powder was cut into six pieces of approximately equal weight. All six pieces were packed into a platinum crucible at the same time and heated to the optimal calcining temperature of 850°C as determined in the preceding experiments. Calcining times of 0.5, 1, 2, 4, 8, and 20 hrs were used. After each length of time, one of the pieces was taken out of the crucible without cooling down the remaining slices. Temperature change as indicated by the control unit was less than 10°C during the removal of a piece.

Every calcined powder sample was crushed with a Lucite mortar and pestle. X-ray powder diffraction patterns were taken on each of the specimens to check the degree of reaction. The patterns obtained showed an almost identical intensity of corresponding peaks. No differences could be observed between the pattern of the sample calcined for 1 hr and the pattern of the sample calcined for 20 hrs. Only the peaks in

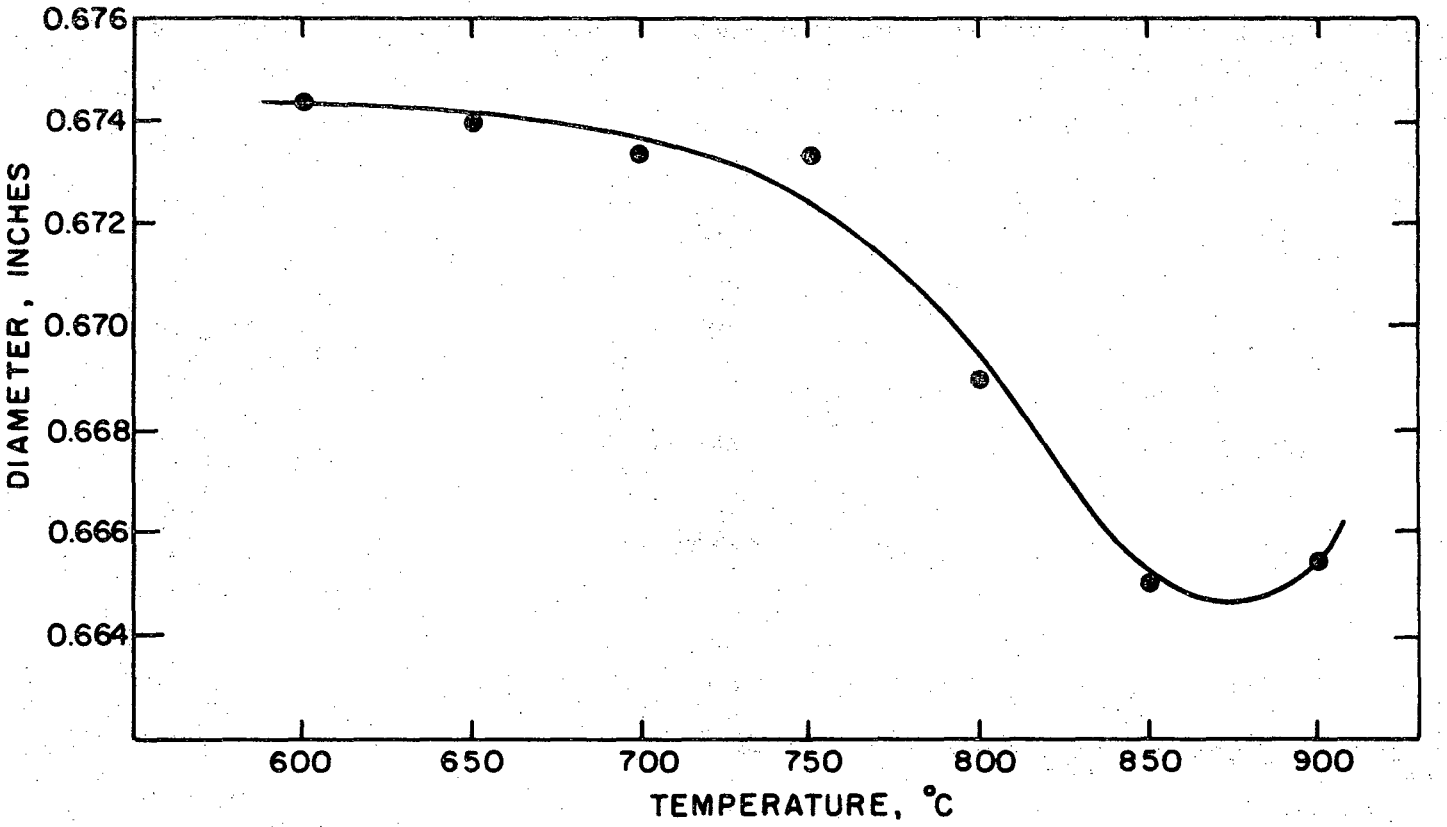

XBL 707-1469

Fig. 7. Diameter of the sintered pellets versus calcining temperature at constant calcining time (2 hrs).

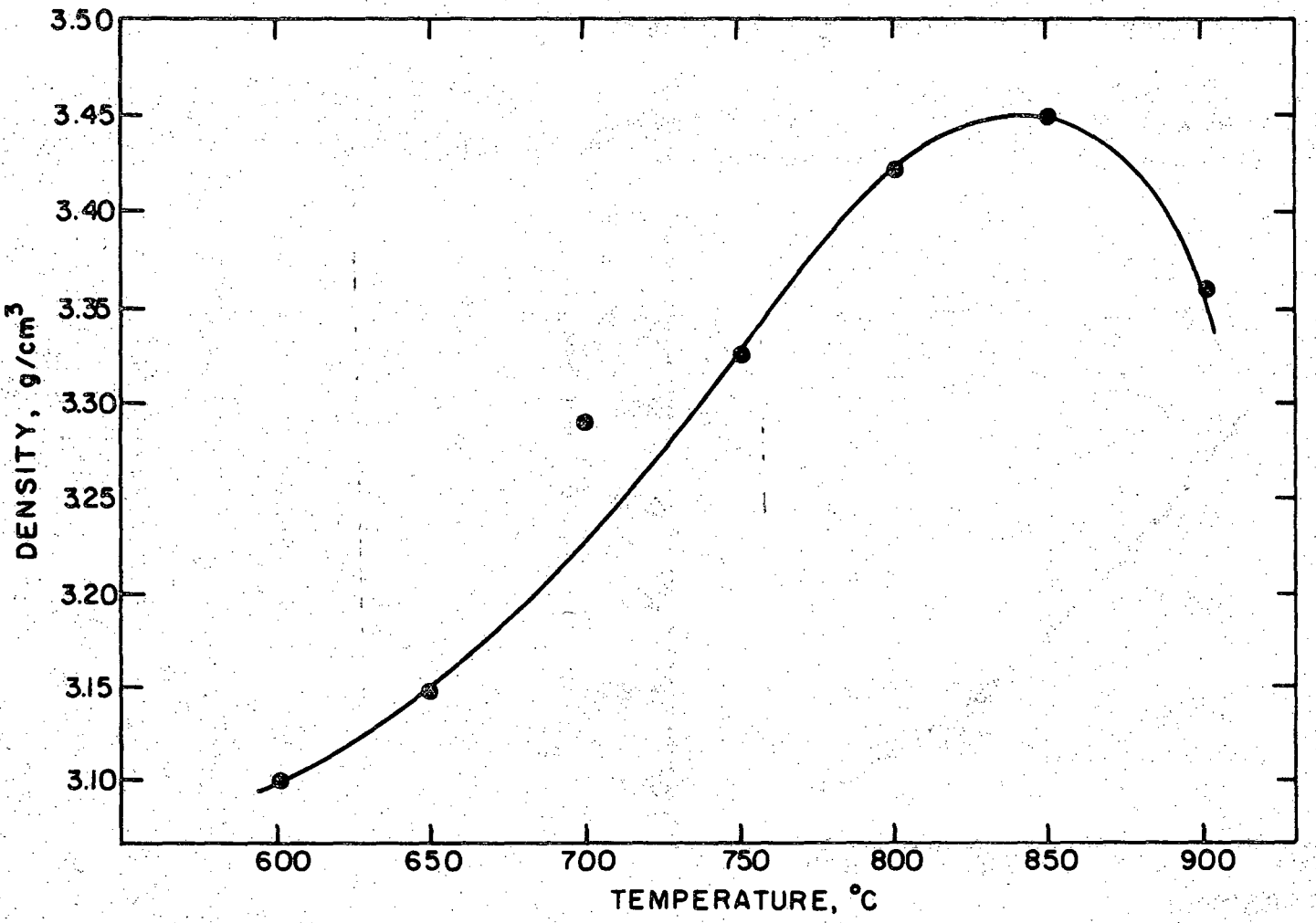

XBL 707-1470

Fig. 8. Density of the sintered pellets versus calcining temperature at constant calcining time (2 hrs).

the pattern of the powder sample calcined for 0.5 hr showed a small broadening of all lines.

The preparation of pellets for the sintering process and the heat treatment at 1050°C for 2 hrs were essentially the same as for the experiments of optimization of calcining temperature. The changes of both the diameter of the pellets and their density were measured and plotted as a function of calcining time. The results are shown in Figs. 9 and 10.

The optimal conditions for calcining in air of sodium-potassium niobate of the composition $(Na_{0.5}K_{0.5})NbO_3$ prepared with carbonates as raw materials have been determined to be

$$T = 850°C$$

$$t = 2 \text{ hrs}$$

The assumption was made that the same conditions will be valid for calcining sodium-potassium niobate prepared with nitrates as raw material. Therefore, all batches have been calcined under these conditions.

After calcining, each batch was dry milled for 24 hrs with the vibratory mill using polyurethane lined containers and teflon balls as grinding media.

Final particle size measurements carried out with "Fishers Sub Sieve Sizer" showed an average particle size of 1.35 μm which remained almost constant through all batches prepared. Measurements of particle sizes employing the scanning electron microscope showed a particle size distribution range between 0.2 and 1.5 μm. Pictures (A) and (B) of Fig. 11 show representative portions of the calcined powders after grinding. The shape of the particles approaches a cubical form as can be seen,

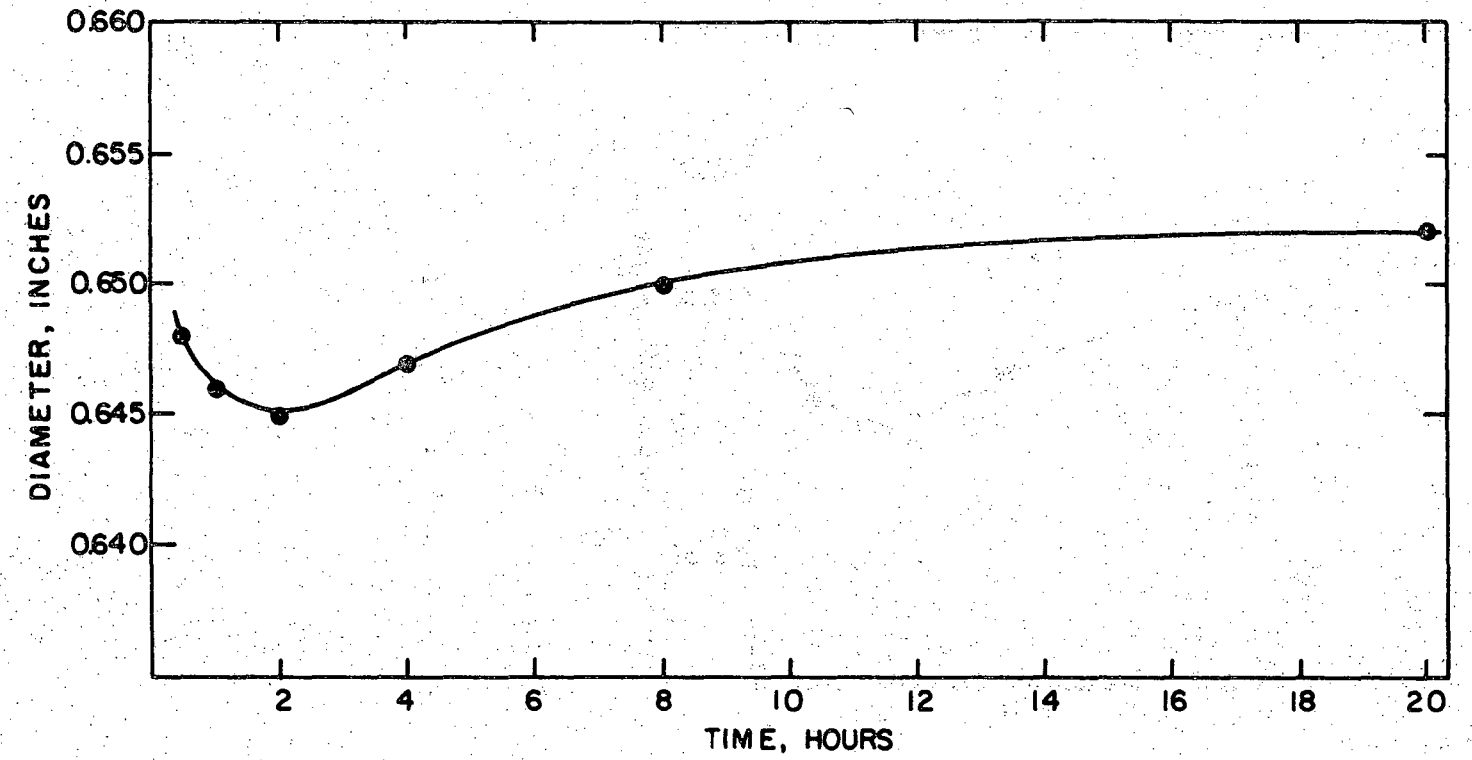

XBL 707-1471

Fig. 9. Diameter of the sintered pellets versus calcining time at constant calcining temperature (850°C).

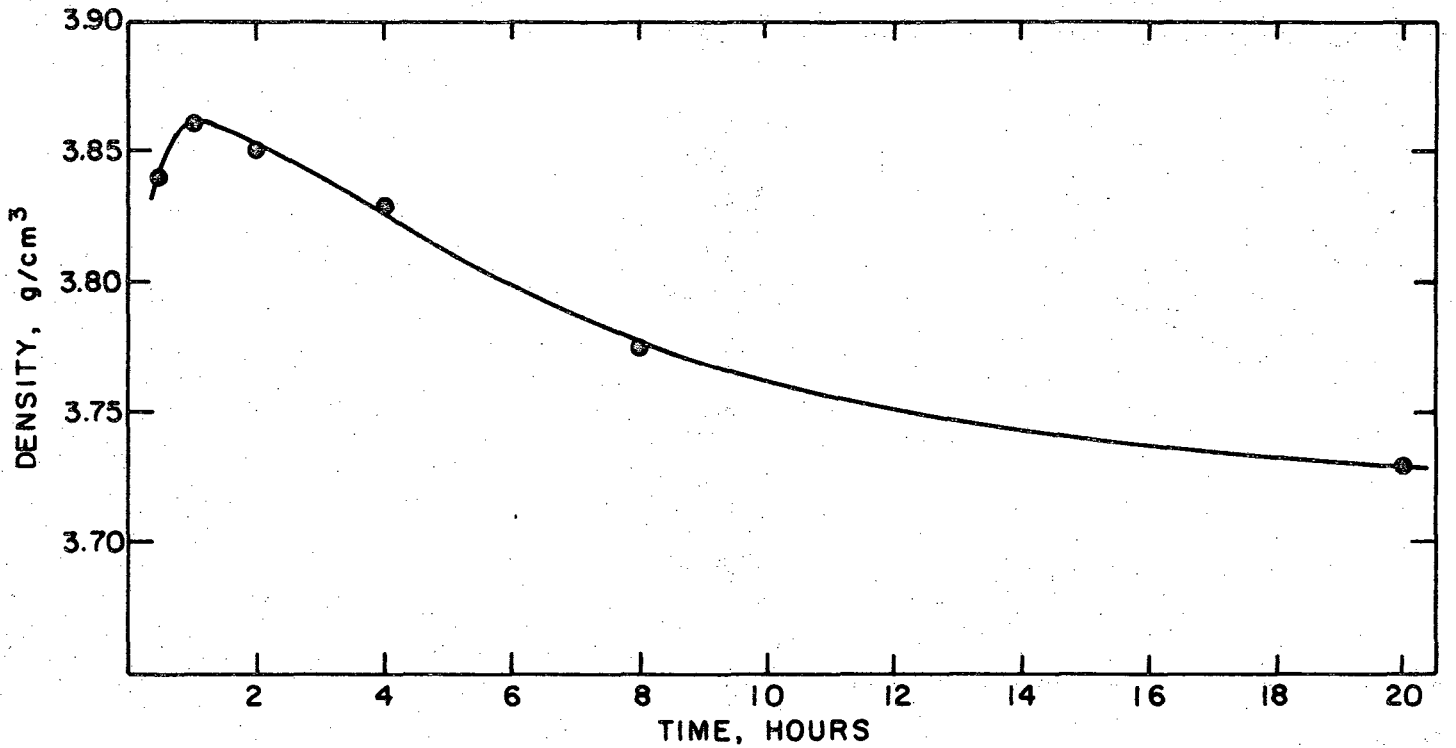

XBL 707-1472

Fig. 10. Density of the sintered pellets versus calcining time at constant calcining temperature (850°C).

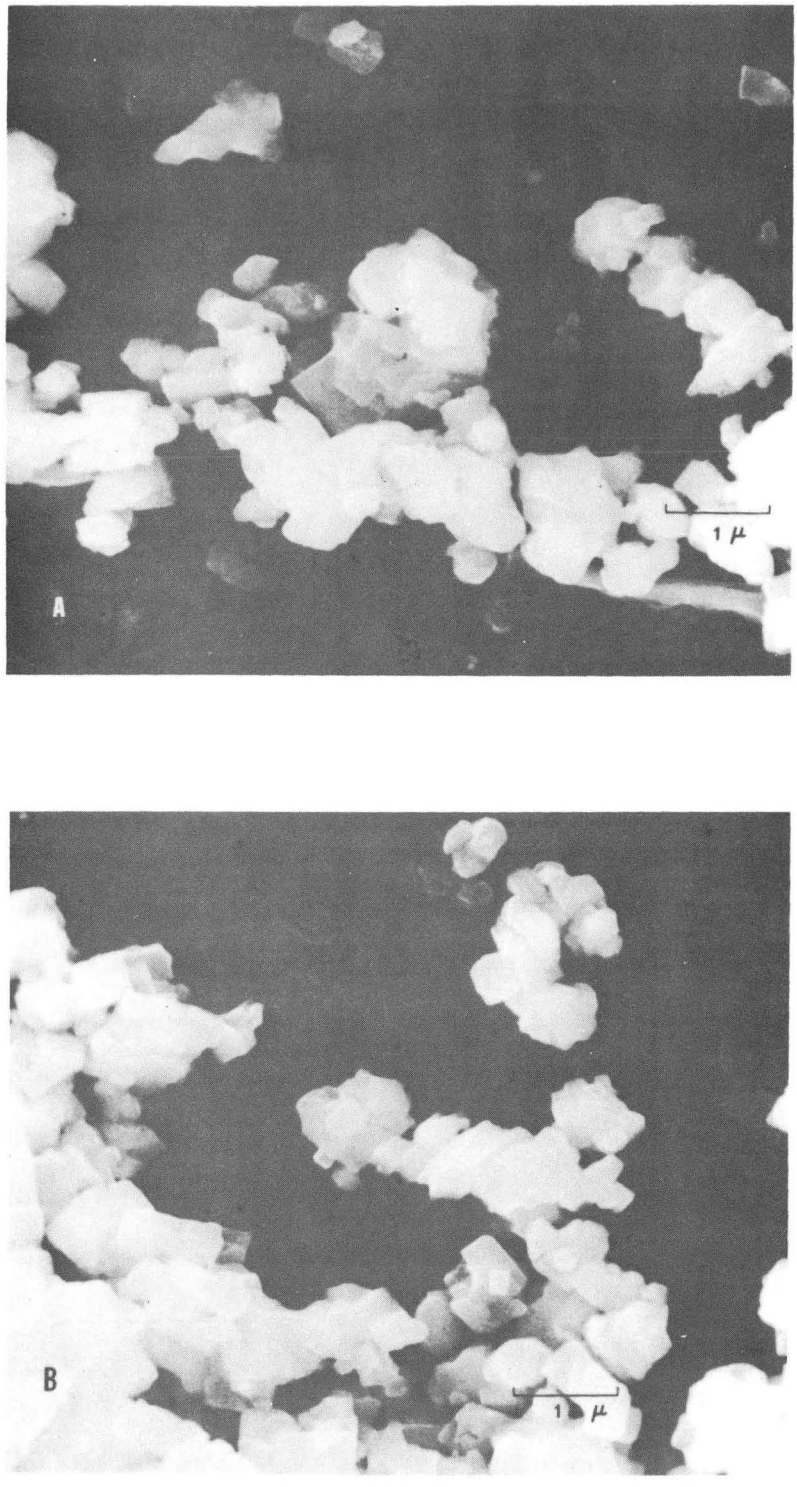

XBB 707-3220

Fig. 11. Scanning electron micrograph of $(Na_{0.5}K_{0.5})NbO_3$ powders after processing.

A. Prepared with carbonates; B. Prepared with nitrates.

particularly in picture (B), of the powder sample prepared with nitrates.

After all processing steps, the sodium-potassium niobate powders were analyzed again by semi-quantitative analysis to determine whether or not their impurity content had increased. The results of some samples are given in Table VI.

Table VI. Results of a semi-quantitative spectrographic analysis* on sodium-potassium niobate samples prepared with carbonates

	Undoped powder sample after calcining 850°C; 2 hrs	0.5% Ba doped powder sample after calcining 850°C; 2 hrs	0.5% Ba doped pellet after sintering 1100°C; 8 hrs
Ba**	0.003	0.4	0.3
Na	12.	8.	12.
K	12.	6.	15.
Mg	<0.001	-	0.001
Al	0.06	0.12	0.12
Si	-	-	-
Ca	0.007	0.005	0.01
V	0.003	0.002	0.002
Fe	<0.01	<0.01	0.01
Cu	<0.02	<0.02	<0.01
Nb	Principal constituent in each sample		

* Reported by American Spectrographic Laboratories, Inc.

** All reported as oxides in wt %.

The prepared sodium-potassium niobate powders were kept in closed polyethylene bottles until further use.

C. Weight Loss Measurements on Stoichiometric $(Na_{0.5}K_{0.5})NbO_3$

The weight loss experiment was conducted in air with the weight change recorded continuously on an automatic microbalance. The sample placed in a platinum crucible suspended from a platinum wire connected to one arm of the microbalance into a Kanthal wound tube furnace. Regulation of temperature was carried out by a variable proportional controller using a control thermocouple at the hottest point of the muffle furnace.

Approximately 320 mg of -115 mesh powder of stoichiometric $(Na_{0.5}K_{0.5})NbO_3$ calcined in the optimal region at a temperature of 850°C for 2 hrs was heated at a rate of 4-5°C per minute under muffled conditions. The final temperature was 1200°C. The measured values are plotted in Fig. 12.

D. Influence of the Sintering Atmosphere on Density and Weight Loss

The high vapor pressures of the alkali oxides at high temperatures suggested a determination of the influence of sintering atmosphere on density and weight loss of the pellets. For this purpose sintering experiments were carried out using pellets of the composition $(Na_{0.5}K_{0.5})NbO_3$ prepared with carbonates. The pellets had 3 mole % excess carbonates.

A sintering run was conducted in air at 1 atm pressure and in pure oxygen gas of 1 atm pressure. Sintering temperature was 1050°C; sintering time 2 hrs. No packing powder was used. The pellets were placed on a sheet of platinum.

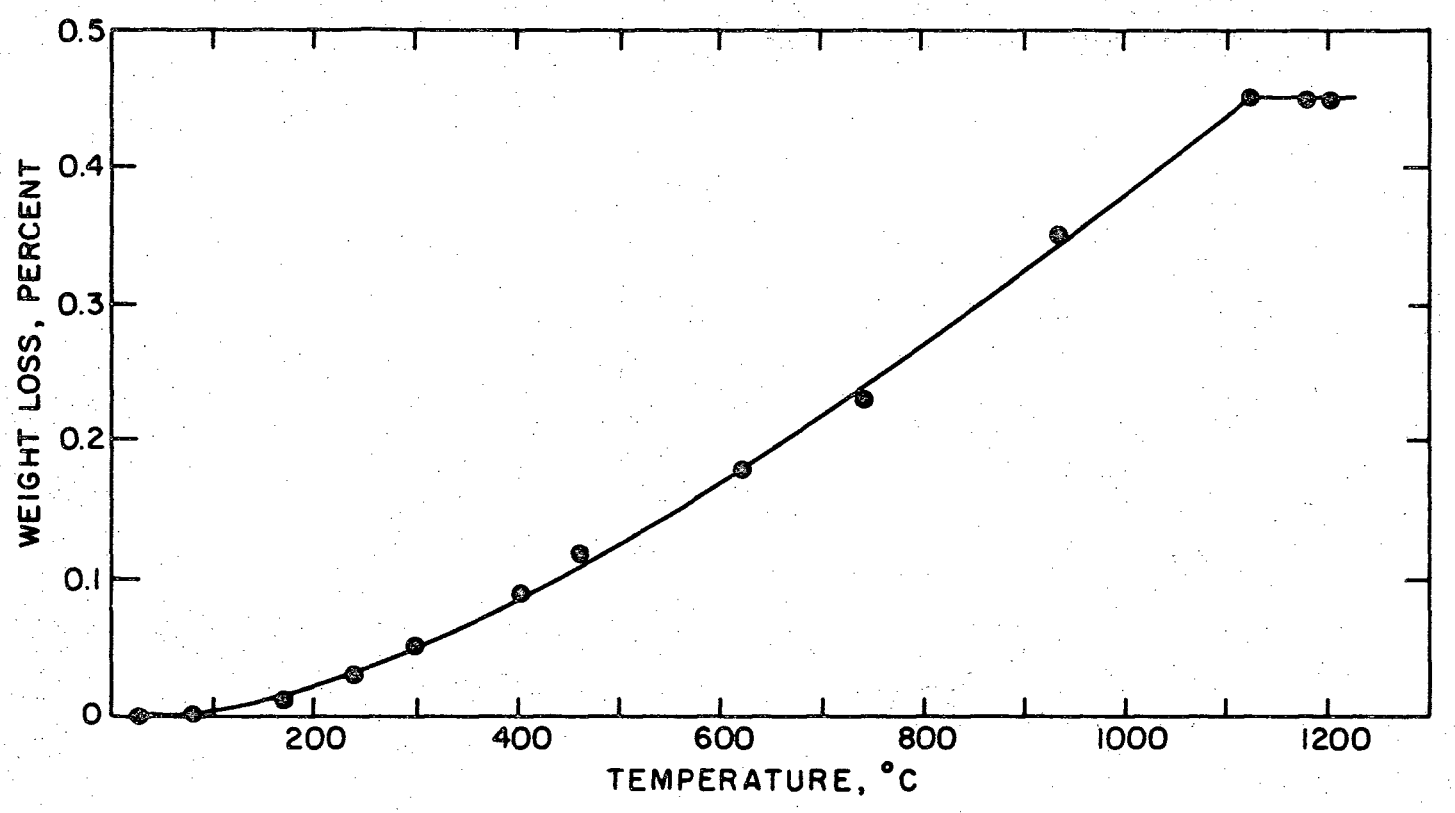

XBL 707-1473

Fig. 12. Weight loss of stoichiometric sodium-potassium niobate.

The pellets sintered in air showed a weight loss of 2.2 weight % and a density of 88.5% of theoretical. The pellets sintered in oxygen showed a weight loss of 1.1 weight % and a density of 92.5% of theoretical.

The diminution of weight loss due to sintering in oxygen atmosphere can be explained by the following reaction

$$Na_2O \rightleftharpoons 2Na + \frac{1}{2} O_2$$

neglecting the influence of higher oxides of sodium such as Na_2O_2 and NaO_2. The equilibrium constant for this reaction is:

$$K_{eq} = \frac{P_{Na}^2 \; P_{O_2}^{1/2}}{P_{Na_2O}}$$

By changing the sintering atmosphere from air to pure oxygen, the partial pressure of oxygen increases by a factor of 5; consequently, the weight loss of sodium has to decrease as can be seen from the equilibrium constant. The same considerations are true for potassium and its oxides.

For this reason, all sintering experiments were conducted in a flowing oxygen atmosphere.

E. Sintering

Pellets of 3/4 inch diameter were cold pressed using a tungsten alloy steel die and a pressure of 20,000 psi. The pellets ranged in weight from 3 to 4 grams. In order to improve the green strength of the pellets, the powder to be pressed was wetted slightly by adding approximately 2 cm^3 isopropyl alcohol to 100 grams of dry powder. Green densities obtained ranged from 61 to 64% of theoretical depending upon

the composition of the powder pressed. The pressing process was followed by a drying step in an electric oven at a temperature of 105°C for 24 hrs to evaporate the added isopropyl alcohol.

For the sintering process the pellets were packed into a cylindrical platinum crucible with a cover. Because of the high vapor pressures of the alkali oxides, it was necessary to use packing powder techniques to provide a sodium and potassium vapor surrounding the pellets. Undoped packing powder of the composition $(Na_{0.5}K_{0.5})NbO_3$ was used having 3 mole % excess in alkali carbonates. The excess in alkali carbonates in the packing powder was chosen to provide a well defined activity of both sodium and potassium through the whole sintering process. This precaution was necessary because of the jump in activities which will occur by going from the sodium and potassium-rich to the sodium and potassium-poor side of the compound $(Na_{0.5}K_{0.5})NbO_3$. This change in activities implies only a small change in composition because of the narrow solid solution range of both the compound $(Na_{0.5}K_{0.5})NbO_3$ and the single niobates $NaNbO_3$ and $KNbO_3$, as can be seen from the phase diagrams of the system K_2O-NbO_3 Fig. 1 and of the system Na_2O-Nb_2O_5 Fig. 2. Such an uncontrolled jump in activities can change the sintering characteristics drastically.

A Kanthal-wound furnace shown in Fig. 13 was used for sintering the pellets. After loading the furnace, it was pumped down to approximately one thousandth of an atmosphere and refilled with oxygen gas. A flowing oxygen atmosphere was established and maintained through the whole firing period. The furnace heating rate was 15°C per minute and the thermal gradient in the hot zone determined in previous measurements was less

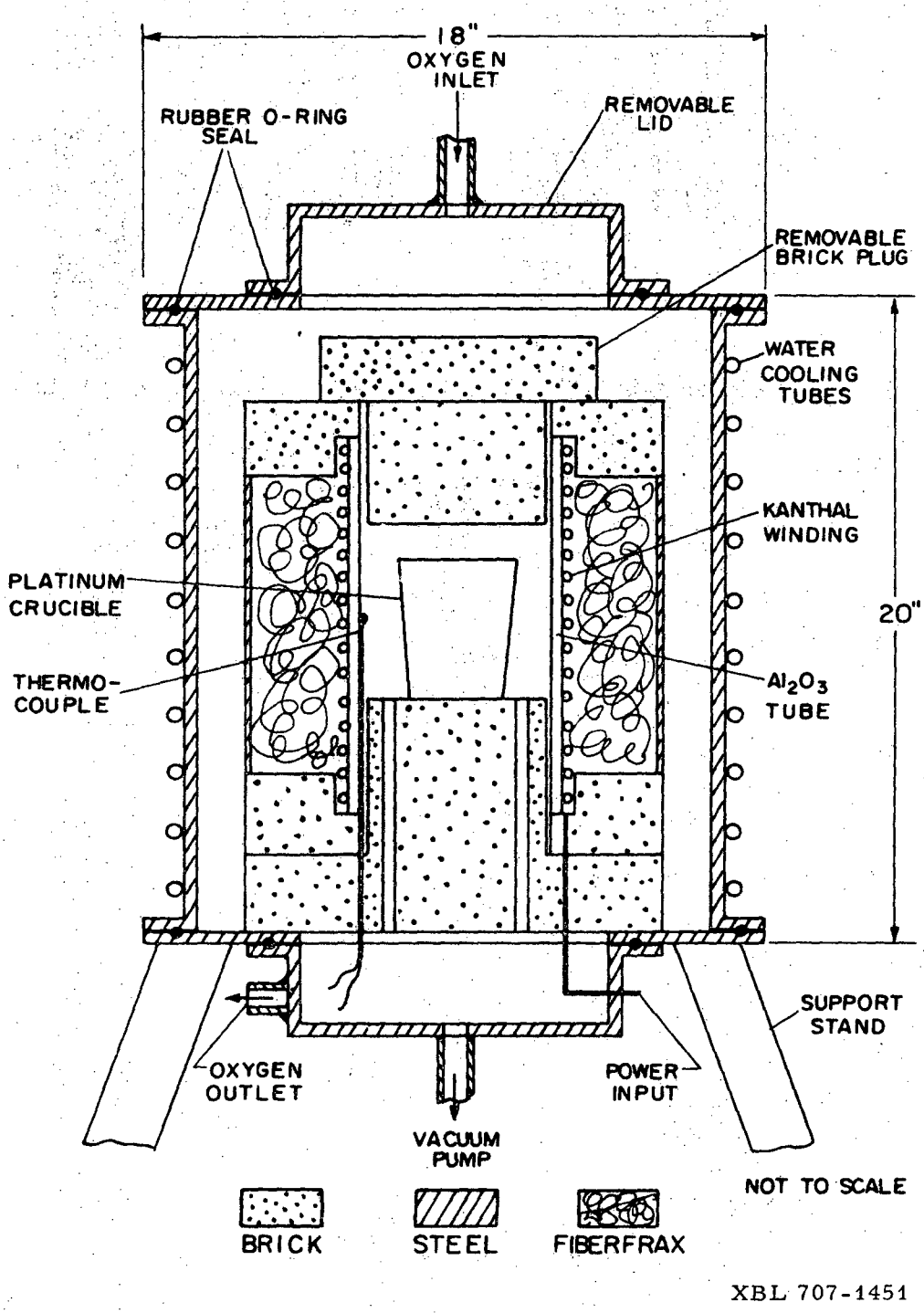

Fig. 13. Furnace used for calcining and sintering.

than ±5°C. After firing, all sintered specimens were quenched in air by removing the crucible from the furnace. As the pellets reached a temperature of about 400°C they were put into a dessicator for further cooling to room temperature. This precaution was necessary because of the hygroscopic nature of some specimens, especially of pellets sintered for short periods of time and of pellets having low densities. Samples with high densities did not appear hygroscopic; even a normal exposure to laboratory atmosphere for several weeks had little effect on the material.

Furthermore, color changes from bright yellow to white were observed as the samples were cooled. High density pellets exposed to white light exhibited photochromatic effects. An exposure of these samples to UV light changed their color to blue. The same color change but much more marked could be obtained by heating the high density samples in air. The color change did not reverse on cooling.

Weight of the packed platinum crucible was determined before and after each firing period. The weight change observed was less than 0.1% weight loss for every event and appeared to be quite constant.

Density measurements were made using a mercury immersion apparatus combined with an Ainsworth balance. Specimens used for density measurements were checked carefully for small cracks. The accuracy of all density measurements is approximately ±0.5%. After finishing these measurements, the specimens were kept in a dessicator.

Figures 14 through 18 show graphs of the relative density plotted versus linear time for specimens prepared with Na_2CO_3, K_2CO_3 and doped with several amounts of $BaCO_3$, whereas Fig. 19 shows a graph with the weight changes plotted versus sintering time of samples sintered at a

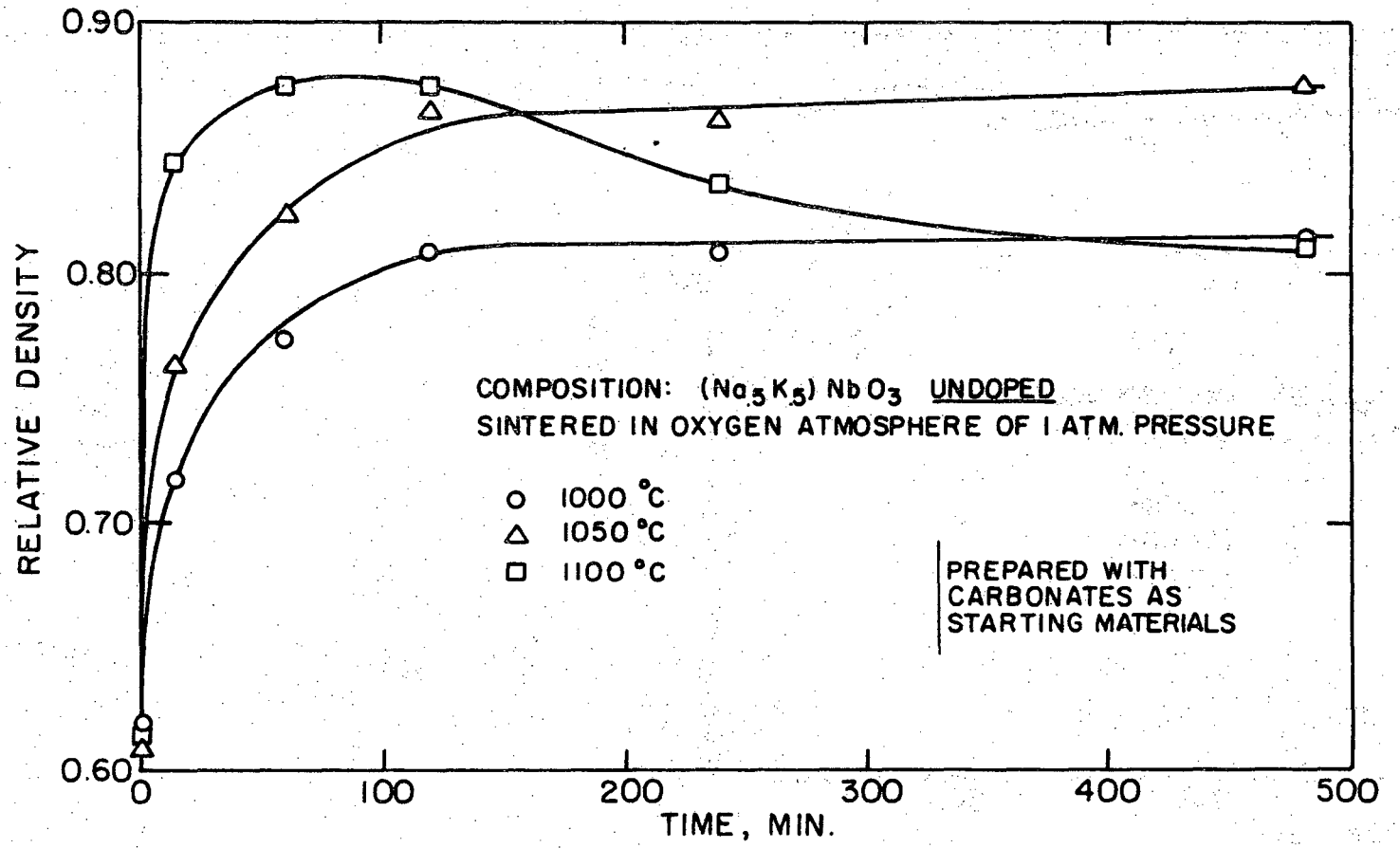

Fig. 14. Relative density of undoped sodium-potassium niobate versus linear sintering time.

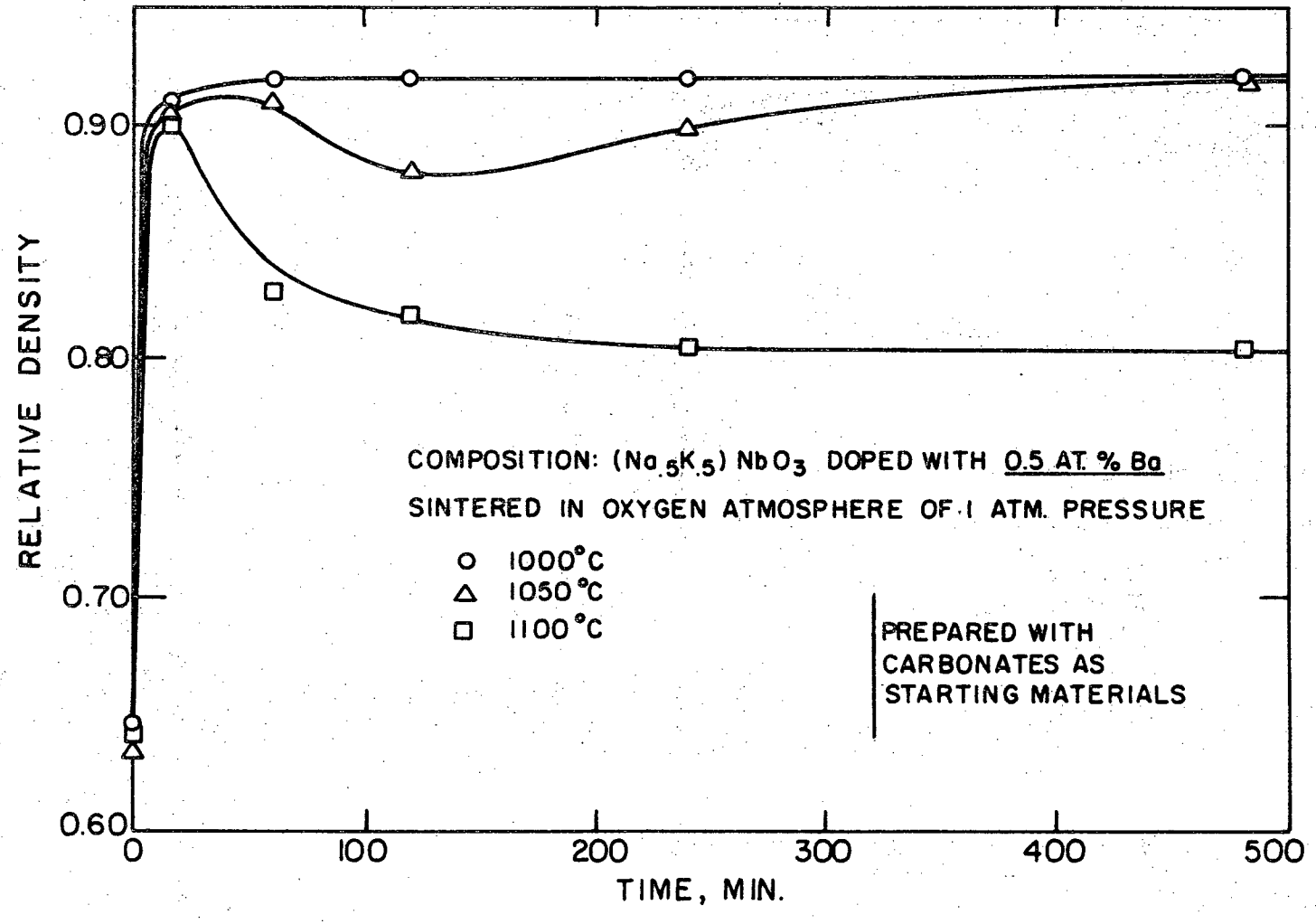

Fig. 15. Relative density of 0.5 atomic % barium doped sodium-potassium niobate versus linear sintering time.

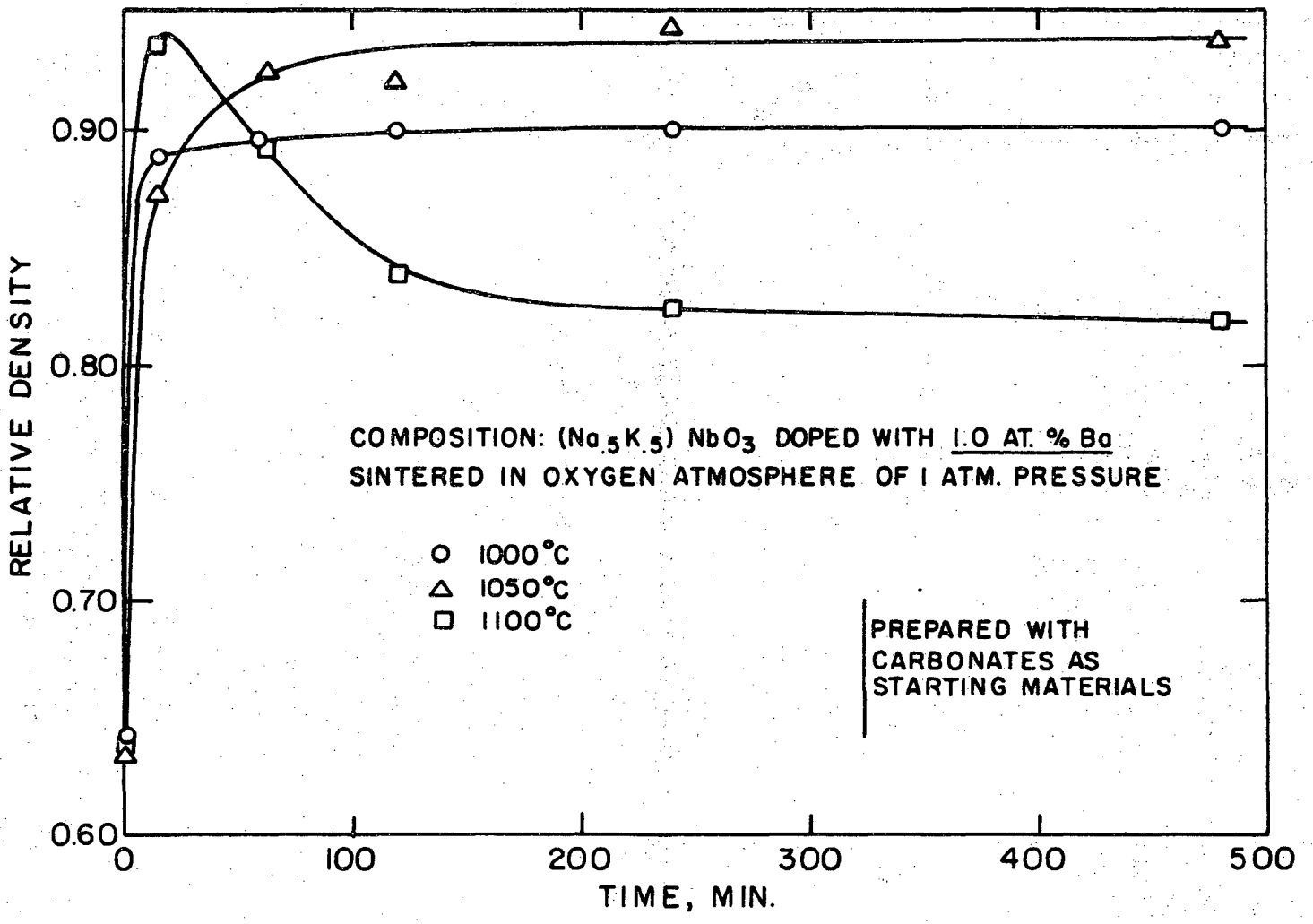

XBL 707-1454

Fig. 16. Relative density of 1.0 atomic % barium doped sodium-potassium niobate versus linear sintering time.

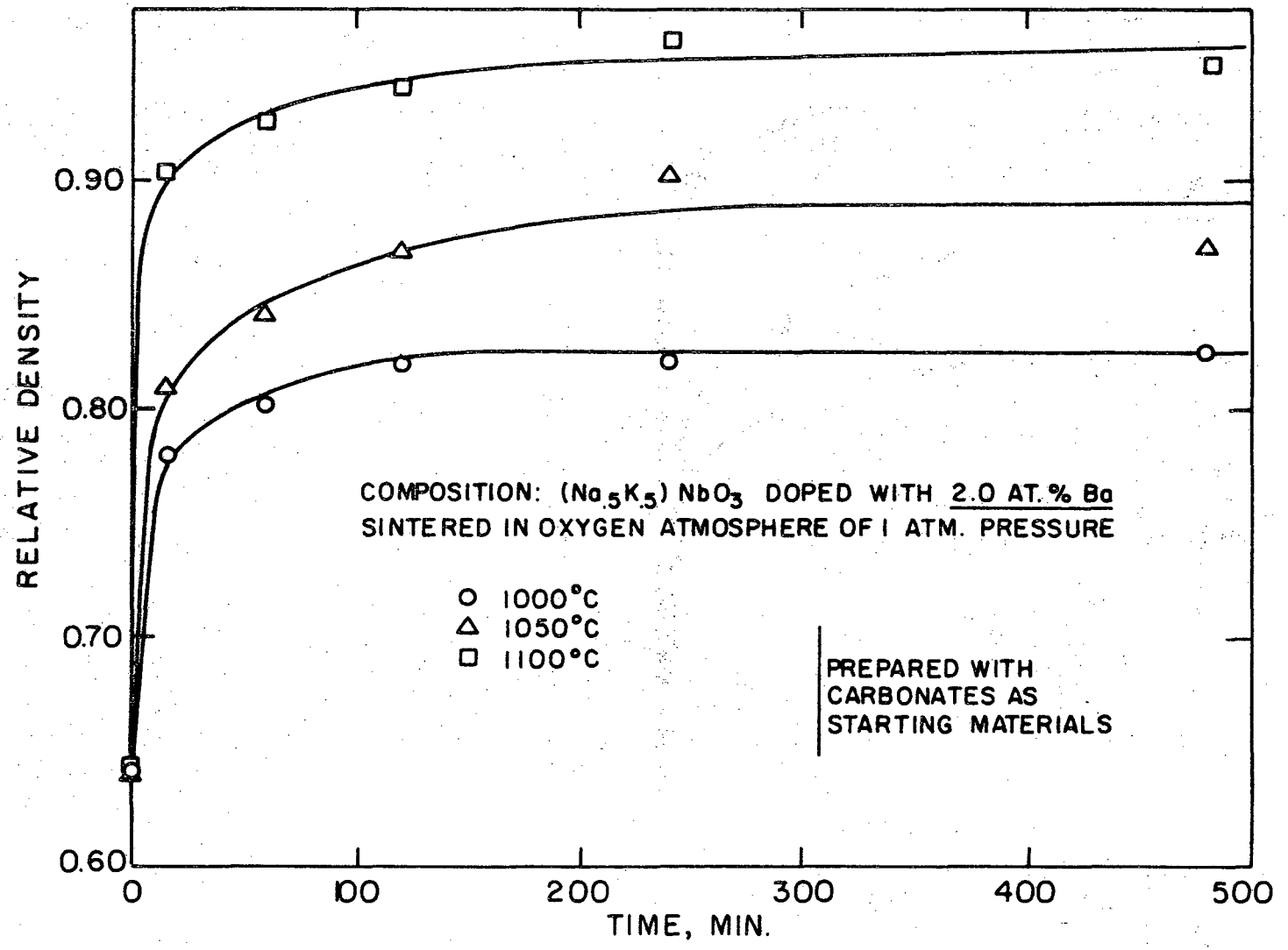

XBL 707-1456

Fig. 17. Relative density of 2.0 atomic % barium doped sodium-potassium niobate versus linear sintering time.

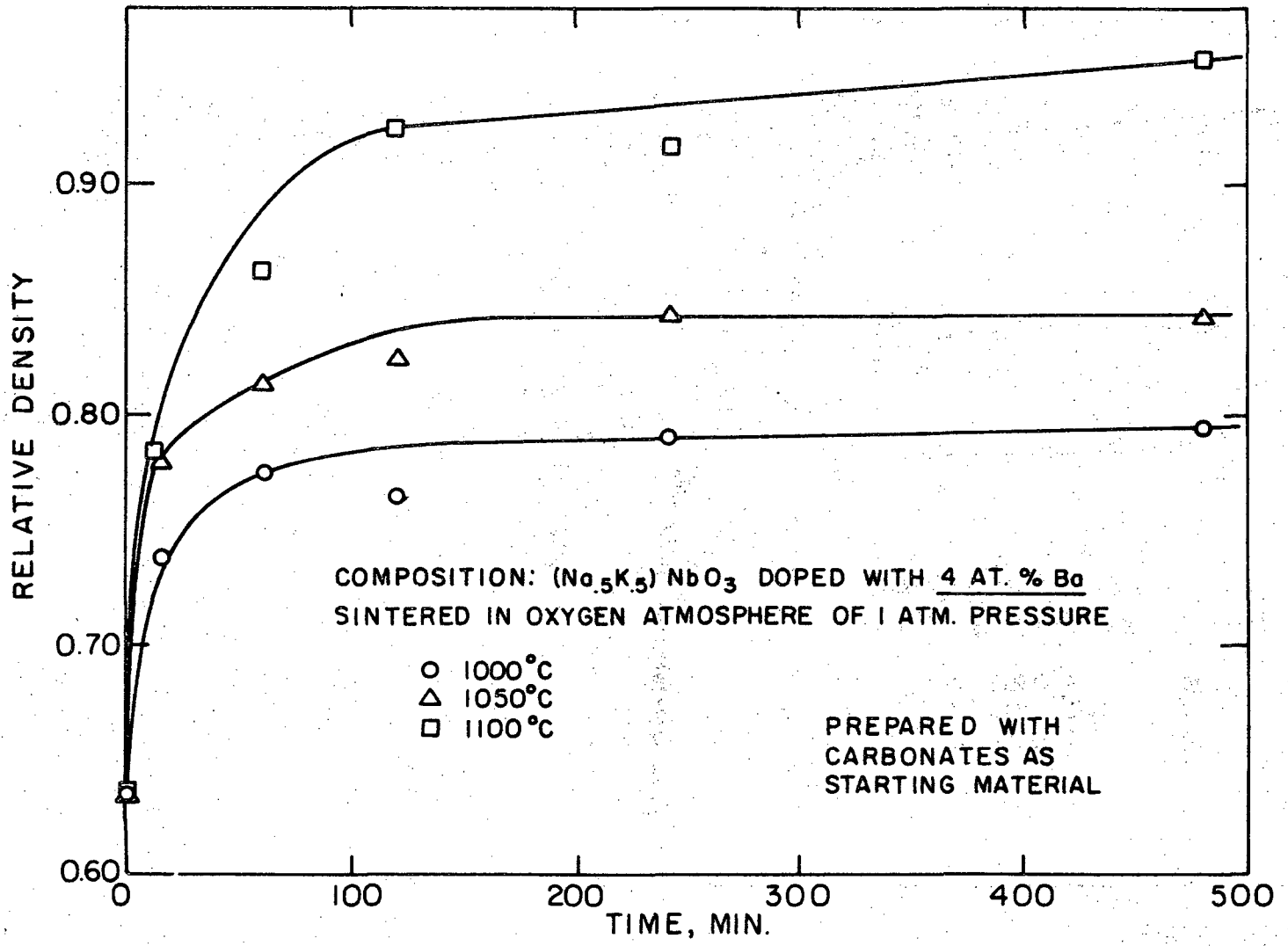

XBL 707-1457

Fig. 18. Relative density of 4.0 atomic % barium doped sodium-potassium niobate versus linear sintering time.

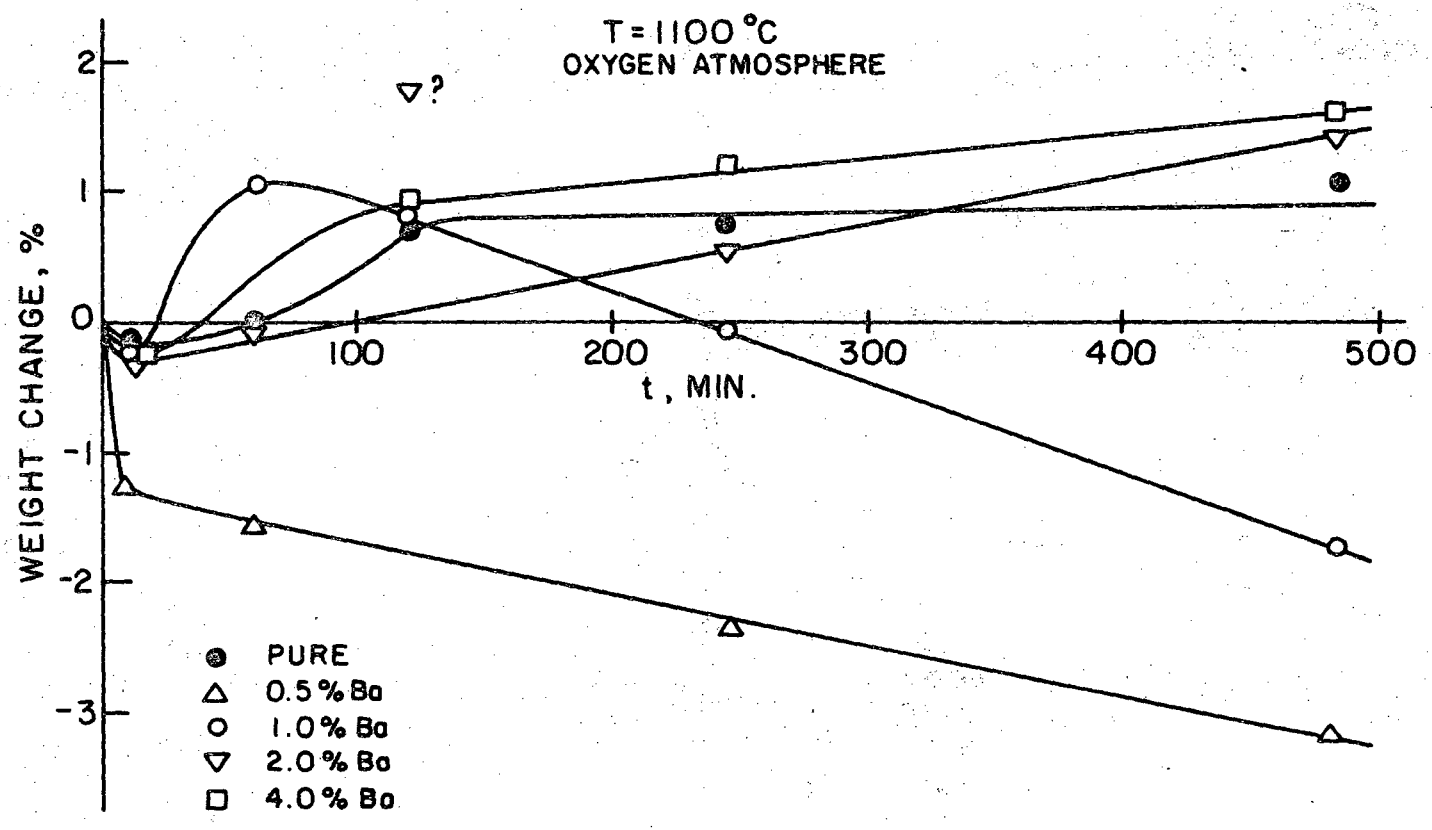

XBL 707-1461

Fig. 19. Weight changes of barium-doped and undoped sodium-potassium niobate prepared with carbonates.

temperature of 1100°C. Figures 20 and 21 show plots of the relative density versus linear time of specimens prepared with $NaNO_3$, KNO_3 and doped with $Ba(NO_3)_2$.

Further sintering experiments were carried out using materials prepared with nitrates having an addition of 5 weight % NaCl. No densification could be obtained even at a temperature of 1100°C and a sintering time of 6 hrs. These samples maintained their green density and showed a weight loss in the range of 5 weight %.

Figure 21 shows a plot of the relative density versus linear time of pellets prepared with nitrates having excess of alkali nitrates. These pellets were sintered at a temperature of 1100°C using a packing powder with a little excess Nb_2O_5. The large difference in the sintering behavior and the density obtained between Fig. 20 and Fig. 21 is caused only by changing the composition of the packing powder from the sodium and potassium-rich to the sodium and potassium-poor side of the compound $(Na_{0.5}K_{0.5})NbO_3$.

F. Electron Probe Microanalysis

A "MAC" Electron Probe Microanalyzer was employed in studying the homogenuity of the sintered pellets with regard to the distribution of sodium, potassium and barium in the bulks. The apparatus was equipped with three scanning dispensive spectrometers which can simultaneously analyze for any element between sodium atomic number 11 and uranium atomic number 92. One of the spectrometers was especially equipped with thin windows and a special analyzing crystal to extend its analyzing range to obtain good data on sodium.

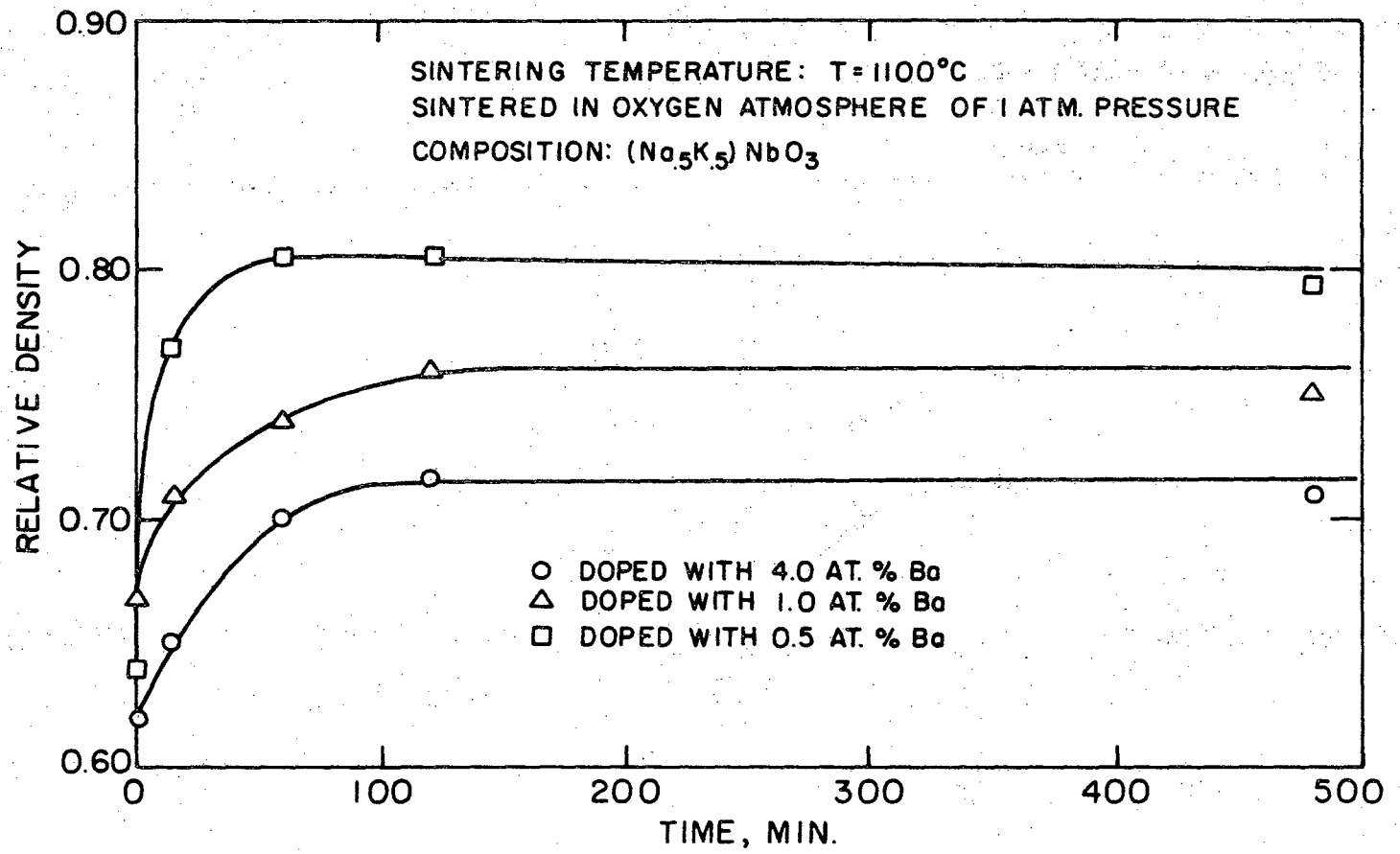

XBL 707-1463

Fig. 20. Relative density versus linear sintering time of barium doped sodium-potassium niobates prepared with nitrates and sintered in packing powder with excess in sodium and potassium.

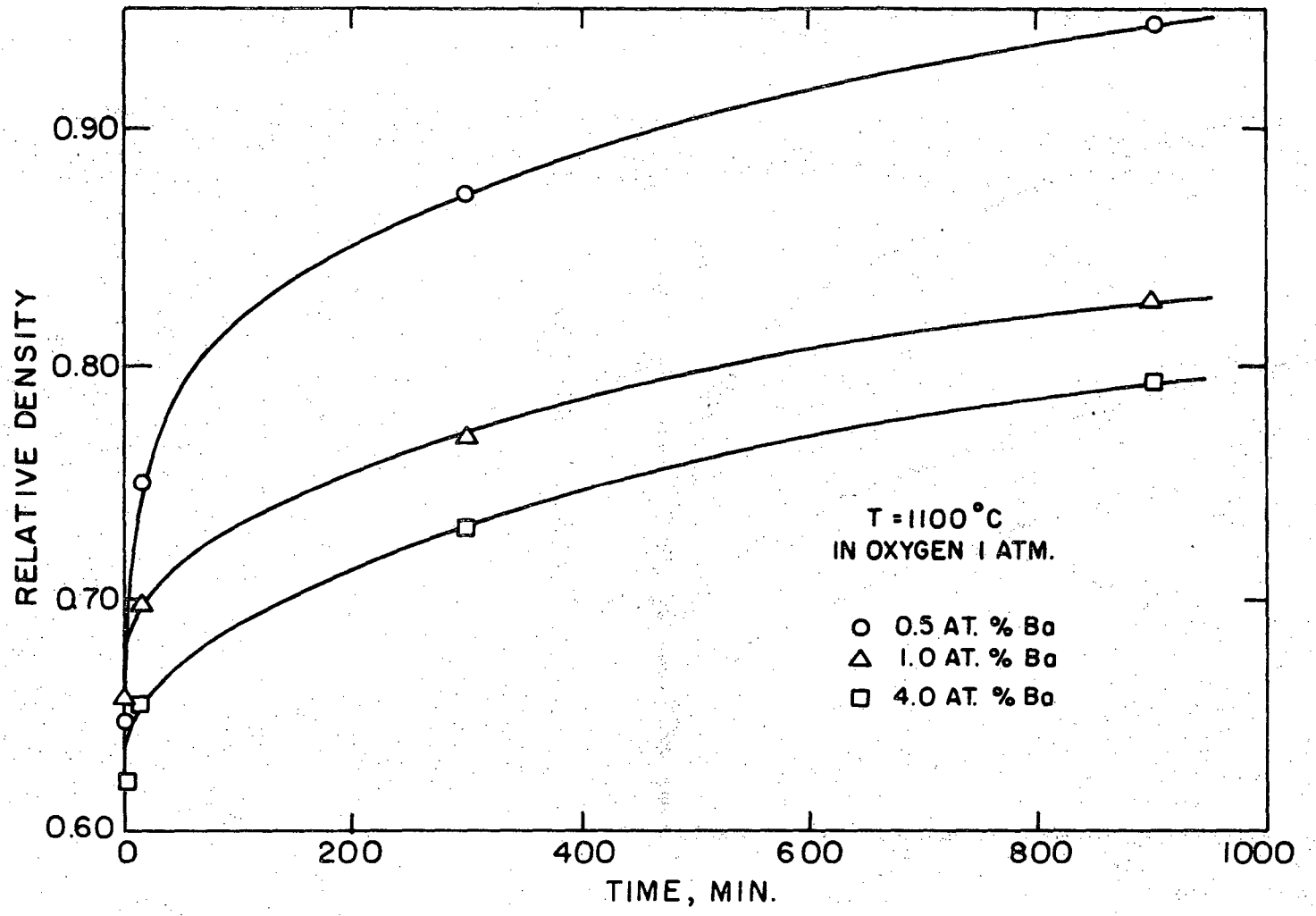

XBL 707-1462

Fig. 21. Relative density versus linear sintering time of barium doped sodium-potassium niobates prepared with nitrates and sintered in packing powder with excess in niobium.

Two samples of each composition prepared were polished and coated with a conductive layer of carbon 100 Å thick. The samples chosen were the pellets possessing the highest density and the pellets sintered for the longest time at the highest sintering temperature (1100°C).

Corresponding areas of each sample were scanned recording the intensities of sodium K_α, potassium K_α and barium L_α radiation as a print out. Because of the very homogeneous distribution of all components recorded, no pictures have been taken.

G. X-Ray Studies

All X-ray examinations were done by X-ray diffractometer methods exclusively. A "Norelco" diffractometer utilizing copper radiation was operated at 35kV and 20 m A. X-ray diffraction patterns were taken from both -115 mesh portions of each calcined powder sample and from polished surfaces of sintered pellets.

The X-ray powder patterns were first used to control the stoichiometry of the calcined powder samples, see Section II-B-1. A scan speed of 1/2° 2 θ per minute provided a sufficiently high resolution for this purpose. Figure 4 shows a pattern with and without correction of sodium and potassium in the calcined powder samples.

The X-ray powder patterns were used secondly to investigate the degree of reaction in the experiments made for optimization of calcining time and temperature. The patterns shown in Figs. 5 and 6 were obtained on -115 mesh powder samples with a scanning speed of 1/2° 2 θ per minute.

Thirdly, the X-ray powder patterns were used to determine the influence of the amount of dopant introduced into the sodium-potassium niobates. Figure 22 shows the changes occurring in the (100 peak due to

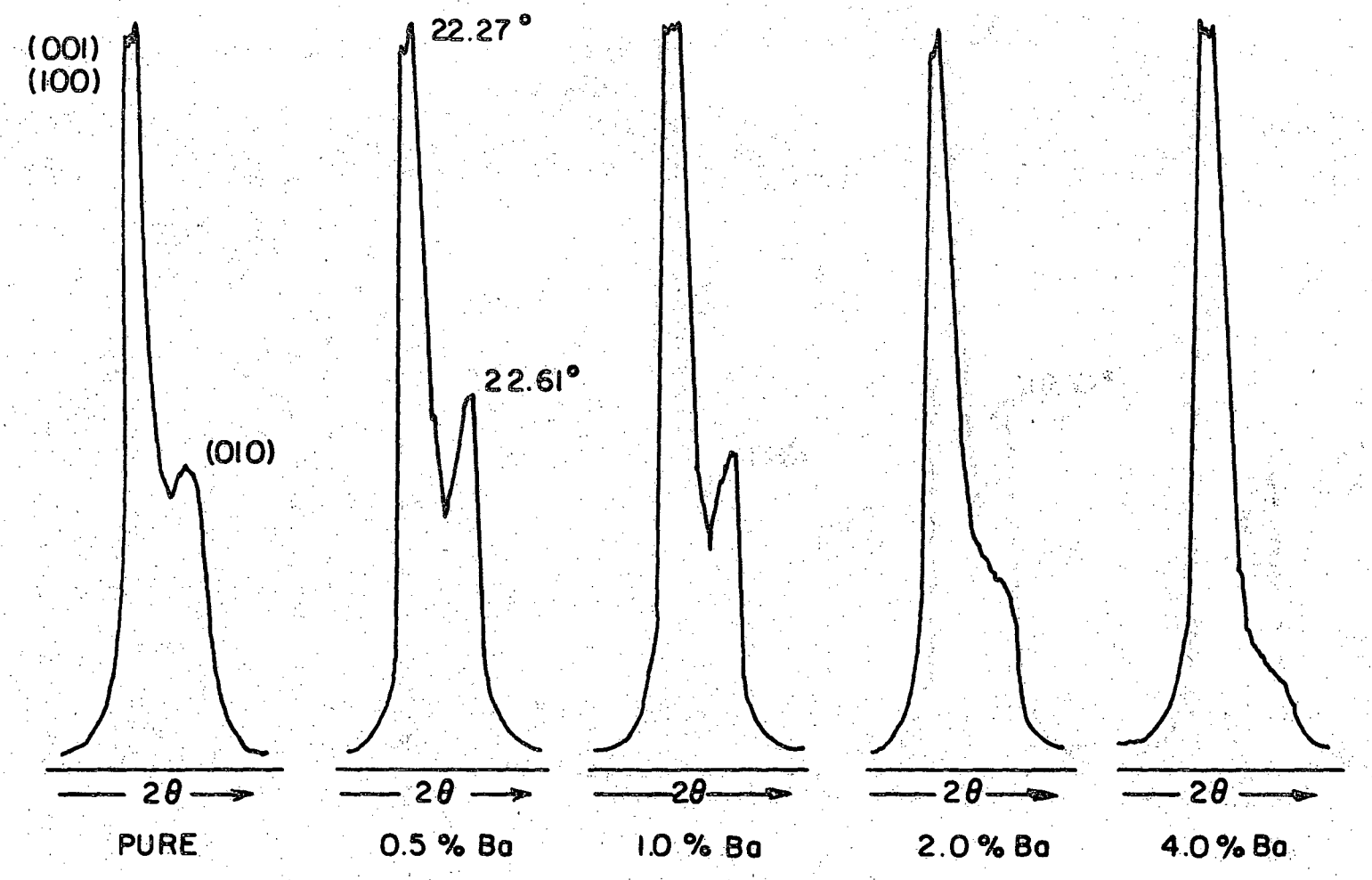

Fig. 22. Intensity change of the {100} peaks due to increasing amounts of dopant (barium).

increasing amount of barium. The peaks are drawn from patterns taken on polished surfaces of sintered pellets with a scanning speed of 1/8° 2 θ per minute.

Fourthly, the X-ray patterns were used for identifying corresponding crystallographic planes (hkl) to all peaks in the pattern and for calculation of the lattice parameters.

1. Indexing the X-ray Diffraction Pattern of $(Na_{0.5}K_{0.5})NbO_3$

For the indexing process, X-ray diffraction patterns were taken on pure and on 4 atomic % barium doped sodium-potassium niobate. The patterns were made using polished surfaces of pellets sintered at a temperature of 1100°C for 8 hrs in oxygen atmosphere. A scan speed of 1/8° 2 θ per minute provided a sufficient resolution of the lines. The peaks of both the doped and undoped material appeared at the same angles; however, differences were observed in the intensities of the lines. Table VII shows the 2 θ values of the peaks and their intensities as observed in the pattern taken on undoped pellets. Furthermore, the corresponding d-spacings and Q-values calculated on basis of the observed d-spacings are listed. Table VIII shows a match of Q-values for all possible planes in the unit cell up to an angle of 2 θ = 84° as calculated on the basis of the Hesse-Lipson plot shown in Fig. 23. All calculations made are based on the assumption of an orthorhombic cell unit having a perovskite type structure as shown in Fig. 24.

The d-spacings as a function of cell edges in an orthorhombic lattice is:[11]

$$d^2_{hkl} = \frac{h^2}{a^2} + \frac{k^2}{b^2} + \frac{l^2}{c^2}$$

Table VII. Evaluation of the patterns taken on an undoped pellet sintered at a temperature of 1100°C for 8 hrs in O_2-atmosphere

Time	2 θ	I (%)	d_p (Å)	Q
1	22.270	80	3.9917	0.06275
2	22.600	40	3.9460	0.06420
3	31.650	60	2.8269	0.12513
4	31.870	100	2.8079	0.12687
5	39.170	3	2.2998	0.18906
6	45.390	57	1.9980	0.25050
7	46.040	8	1.9713	0.25732
8	51.020	17	1.7900	0.31204
9	51.210	24	1.7838	0.31427
10	51.675	7	1.7690	0.31955
11	56.525	36	1.6282	0.37720
12	65.925	12	1.4169	0.49310
13	66.590	17	1.4043	0.50707
14	70.640	7	1.3334	0.56244
15	71.120	9	1.3256	0.56907
16	75.121	13	1.2646	0.62530
17	76.150	2	1.2500	0.64000
18	79.550	2	1.2049	0.68880
19	84.075	6	1.1513	0.75544
20	84.300	6	1.1487	0.75783

Table VIII. Match of observed lines with calculated Q-values using Hesse-Lipson plot for all possible planes of the orthorhombic unit cell up to an angle of 2 θ = 84°

Plane	Q Calculated	# of lines observed	Plane	Q Calculated	# of lines observed
001	0.0625	1	121	0.3820	11
100	0.0627	1	202	0.5008	12
010	0.0642	2	022	0.5068	13
101	0.1253	3	220	0.5078	13
011	0.1267	4	003	0.5625	14
110	0.1269	4	300	0.5643	14
111	0.1894	5	212	0.5650	14
002	0.2500	6	122	0.5695	15
200	0.2508	6	221	0.5701	15
020	0.2568	7	030	0.5778	15
102	0.3127	8	103	0.6252	16
201	0.3133	8	013; 301	0.6268	16
012	0.3142	9	310	0.6285	16
210	0.3150	9	031; 130	0.6405	17
021	0.3193	10	113	0.6894	18
120	0.3195	10	311	0.6910	18
112	0.3769	11	131	0.7030	18
211	0.3775	11			

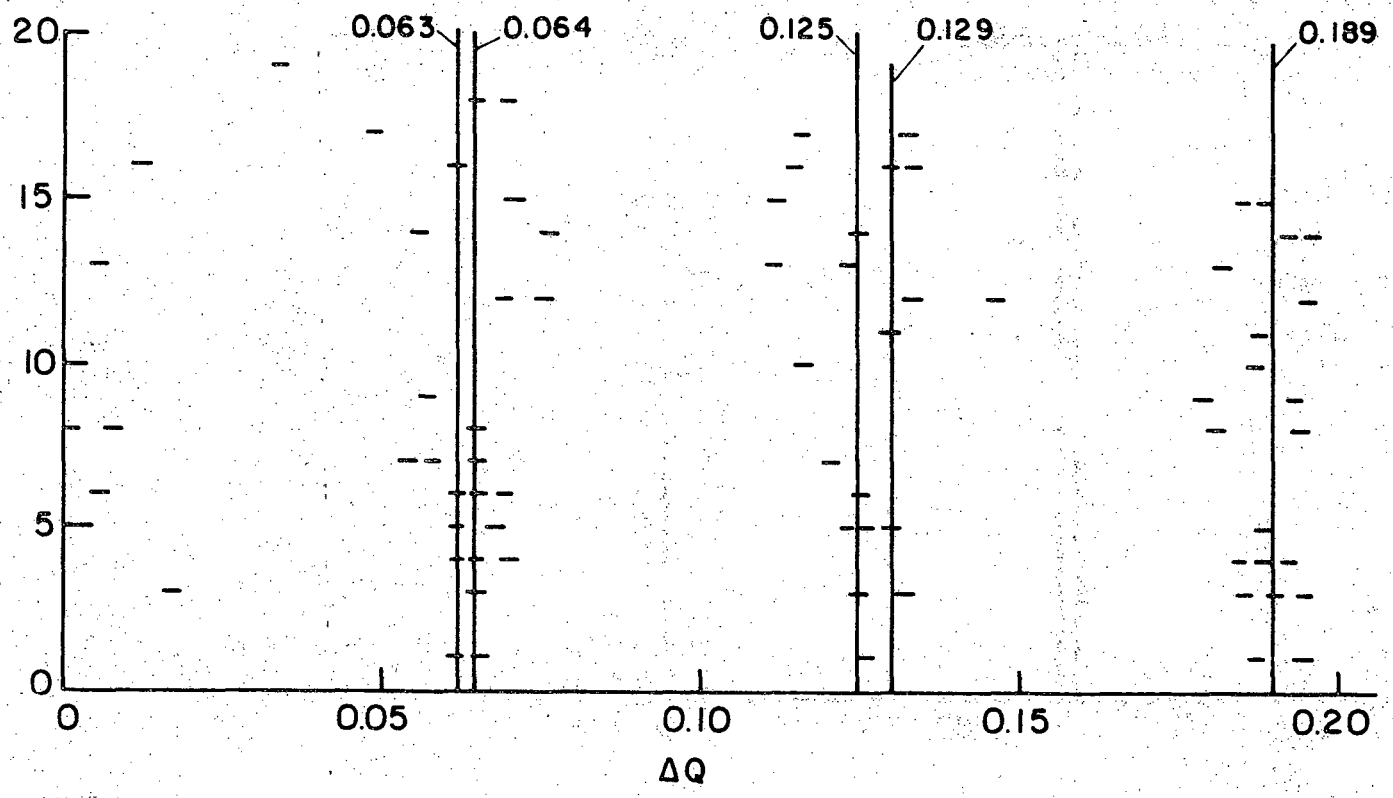

Fig. 23. Hesse-Lipson plot for the orthorhombic unit cell of $(Na_{0.5}K_{0.5})NbO_3$.

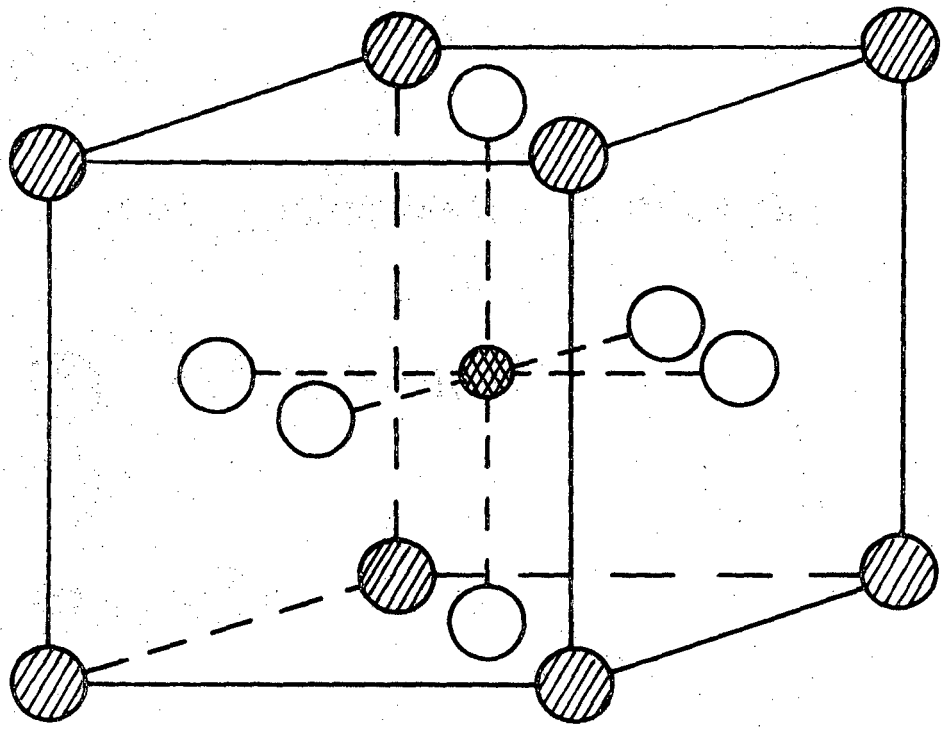

CUBIC PEROVSKITE STRUCTURE

A $Na^{1+}, K^{1+}, (Ba^{2+})$

O O^{2-}

B Nb^{5+}

XBL 707-1452

Fig. 24. Unit cell of $(Na_{0.5}K_{0.5})NbO_3$.

or as a function of reciprocal-cell edges:

$$\frac{1}{d^2_{hkl}} = h^2 a^{*2} + k^2 b^{*2} + l^2 c^{*2}$$

The quantity

$$Q_{hkl} = \frac{1}{d^2_{hkl}}$$

is the dot product of a reciprocal lattice vector with itself.

$$Q_{hkl} = h^2 a^{*2} + k^2 b^{*2} + l^2 c^{*2}$$

Because of the linearity of this relation, it is possible to form different equations of the type

$$Q_{h_1k_1l_1} - Q_{h_2k_1l_1} = \Delta h^2 a^{*2}$$

Table IX contains the ΔQ values calculated for all peaks observed in the pattern. The Hesse-Lipson plot examines the frequency of recurrences of certain ΔQ-values. An evaluation of this plot gives the following lattice parameters for the unit cell of $(Na_{0.5}K_{0.5})NbO_3$.

$$Q_{100} = 1^2 \times a^{*2} = 0.0627$$
$$Q_{010} = 1^2 \times b^{*2} = 0.0642$$
$$Q_{001} = 1^2 \times c^{*2} = 0.0025$$

$$a = 3.99 \text{ Å}$$
$$b = 3.95 \text{ Å}$$
$$c = 4.01 \text{ Å}$$

Table IX. ΔQ-values as calculated from d-spacings observed on a sample of undoped sodium-potassium niobate

	Q	1	3	4	5	6	7	8	9	10	11	12	13	14	15	16	17	18	19
1	.06275																		
3	.12513	.06238																	
4	.12687	.06412	.00747																
5	.18906	.12631	.06393	.06219															
6	.25050	.18775	.12537	.12363	.06144														
7	.25732	.19457	.13219	.13045	.06826	.00682													
8	.31269	.24934	.18513	.18522	.12303	.06159	.05477												
9	.31427	.25152	.18914	.18740	.12521	.06377	.05695	.00218											
10	.31955	.25680	.19442	.19268	.13049	.06905	.06223	.00746											
11	.37720	.37445	.25207	.25033	.18814	.12670	.11988	.06511	.05765										
12	.49310	.43035	.36797	.36623	.30404	.24260	.23578	.18101	.17883	.11590									
13	.50707		.38194	.38020	.31801	.25657	.25387	.19498	.19280	.18752	.12987								
14	.56744				.37338	.31194	.30512	.25035	.24817	.24289	.18752	.06934							
15	.56907					.31857	.31175	.25698	.25480	.24952	.19187	.07590	.00663						
16	.62530						.36798	.31321	.31103	.30575	.24810	.13220	.11823	.05623					
17	.64000							.32791	.32573	.32045	.26280	.14690	.13293	.07756	.07090	.11470			
18	.68880								.37453	.36925	.31160	.19570	.18173	.12636	.11980	.06350	.04880		
19	.75443										.37723	.26113	.24736	.19199	.18536	.12913	.11443	.06563	
20	.75780											.26470	.25073	.19536	.18873	.13250	.13250	.06900	.00337

Calculations using these lattice constants reproduced every peak in the pattern but they are not values obtained by precision lattice constant measurements. A fully indexed pattern is given in Fig. 25.

H. Scanning Electron Microscopy

Investigations were made with a "Jeolco" scanning electron microscope. All pictures were taken from fractured surfaces of sintered pellets. The samples glued with silver paint on the specimen holder were coated with a platinum-paladium layer having a thickness of 100 Å.

The first series of pictures in Fig. 26 show the decrease of grain size caused by the increase of Ba introduced into the material. These pictures were taken from pellets prepared with carbonates and sintered at a temperature of 1100°C for 8 hrs.

Figure 27 shows the analogous series of pictures for a material prepared with nitrates.

The series of pictures in Fig. 28 show the grain growth sqeuence related to the sintering time for materials prepared with carbonates. Because of the very inhomogenous grain growth, no average grain size has been determined.

Pictures shown in Fig. 29 show some details of crystal growth.

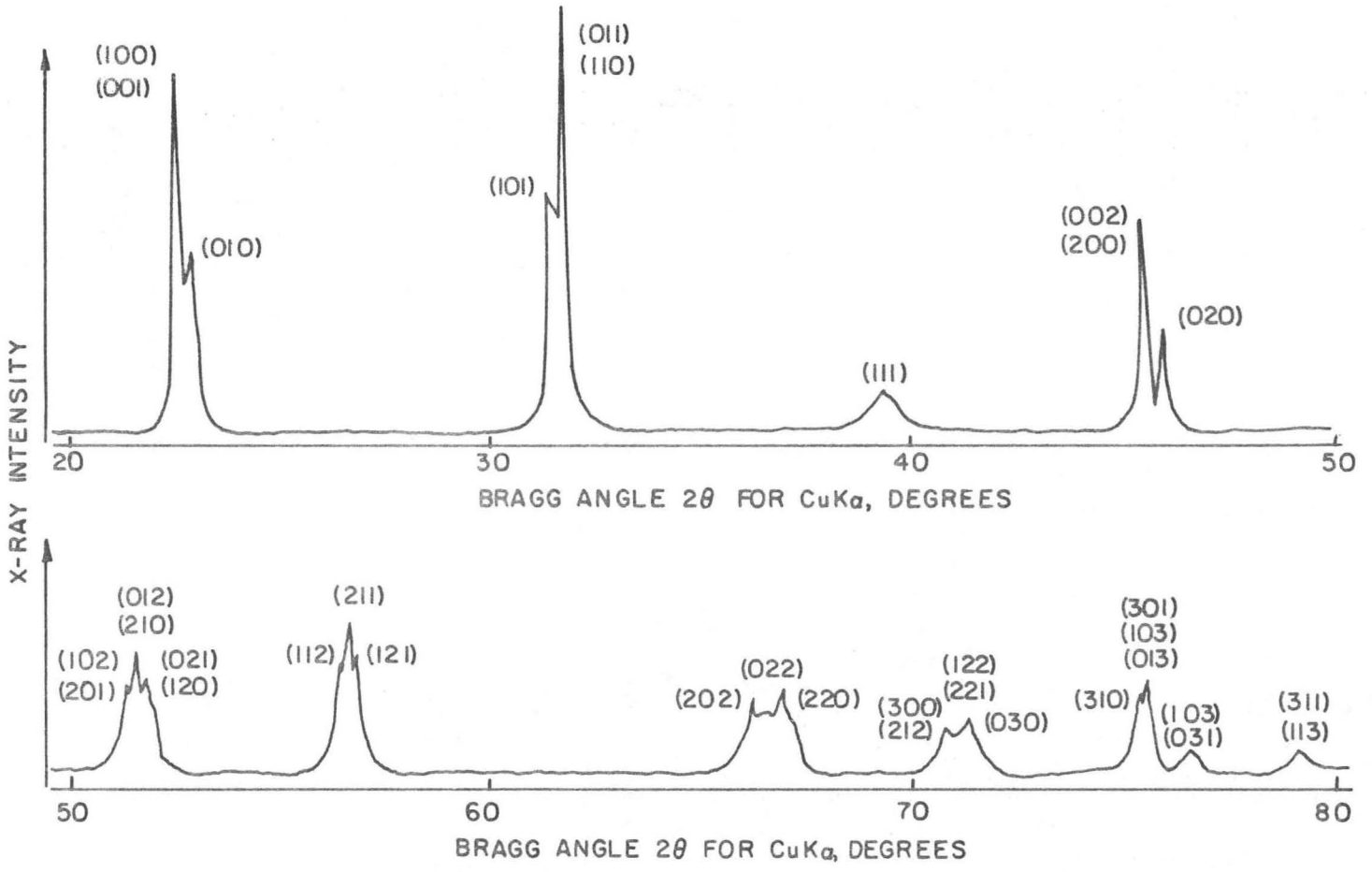

XBL 707-1458

Fig. 25. Index X-ray powder diffraction pattern of $(Na_{0.5}K_{0.5})NbO_3$.

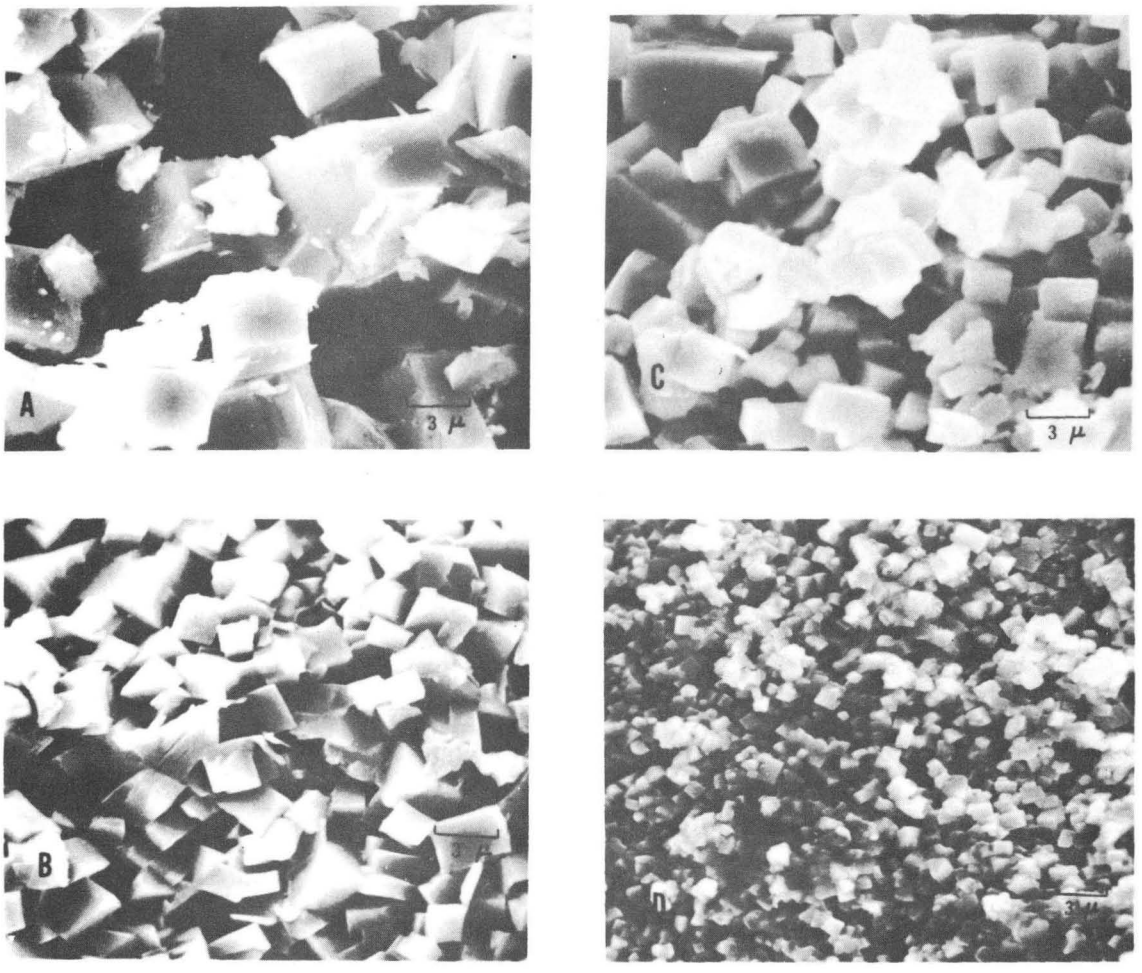

XBB 707-3219

Fig. 26. Scanning electron micrograph showing decrease of grain size due to an increasing amount of barium doped into material prepared with carbonates.

A. undoped, sintered at 1100°C for 8 hrs.
B. 0.5 at. % Ba, sintered at 1100°C for 8 hrs.
C. 2.0 at. % Ba, sintered at 1100°C for 8 hrs.
D. 4.0 at. % Ba, sintered at 1100°C for 8 hrs.

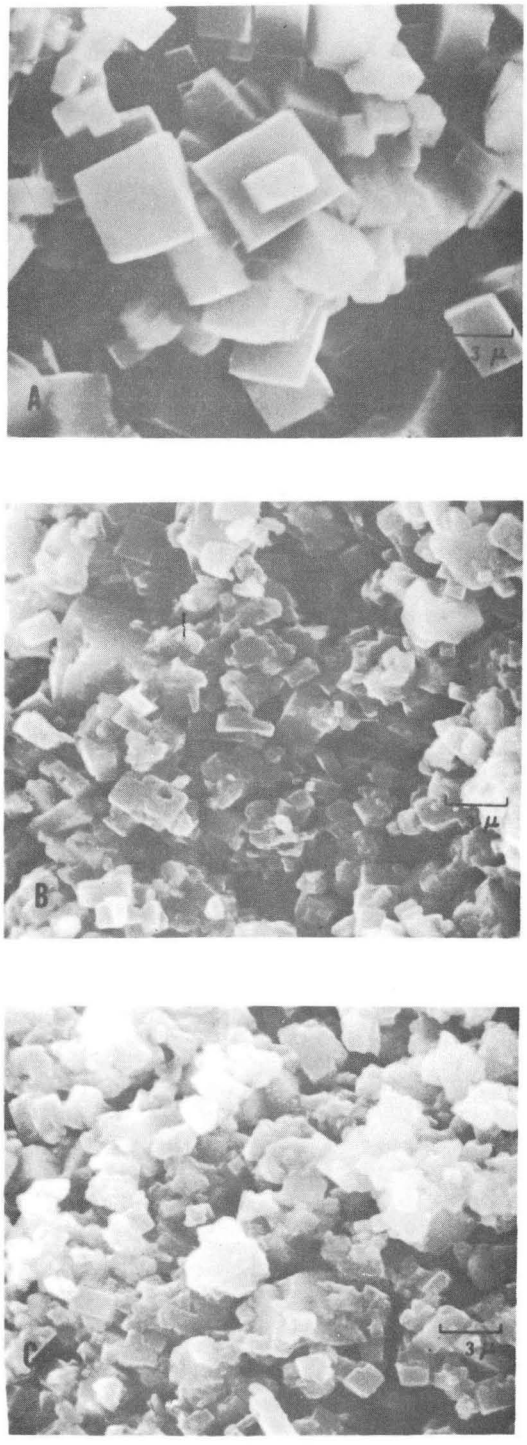

XBB 707-3221

Fig. 27. Scanning electron micrograph showing decrease of grain size due to an increasing amount of barium doped into material prepared with nitrates.

A. 0.5 at. % Ba, sintered at 1100°C for 8 hrs.
B. 1.0 at. % Ba, sintered at 1100°C for 8 hrs.
C. 4.0 at. % Ba, sintered at 1100°C for 8 hrs.

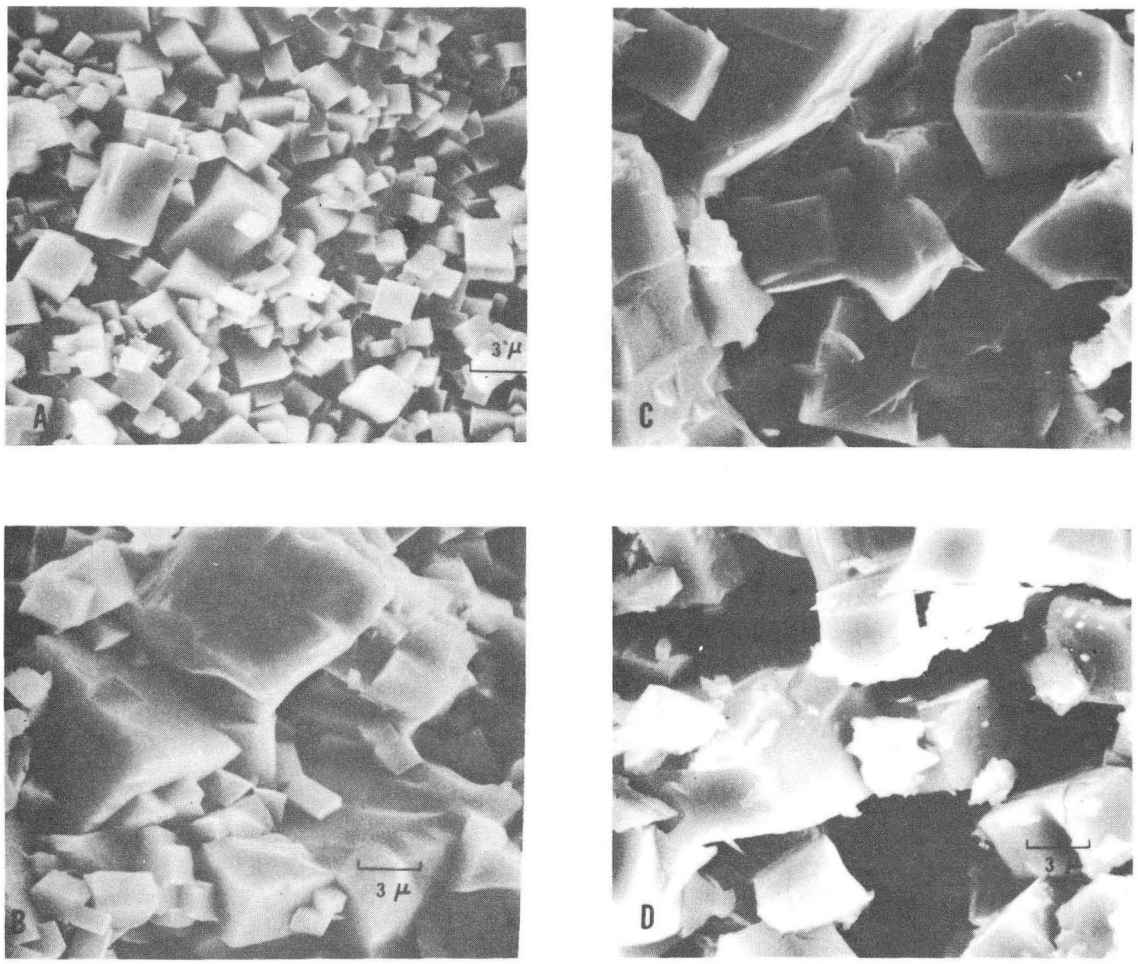

XBB 707-3218

Fig. 28. Scanning electron micrograph showing grain growth behavior of undoped sodium-potassium niobate sintered at 1100°C for

A. 15 min

B. 1 hr.

C. 4 hrs.

D. 8 hrs.

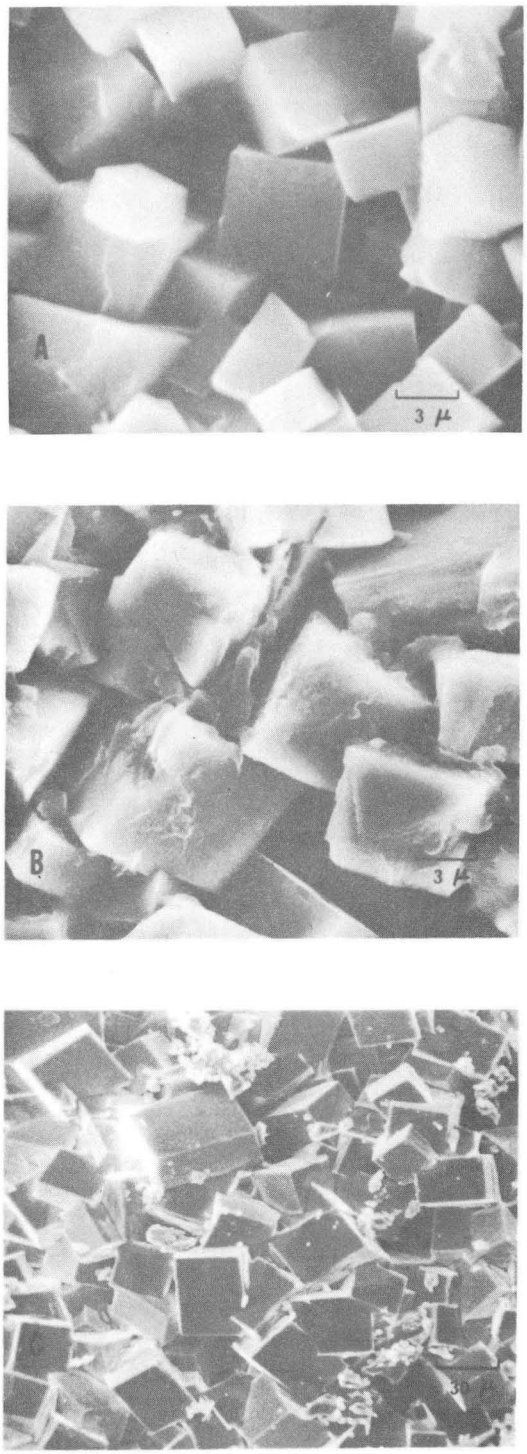

XBB 707-3217

Fig. 29. Crystals grown in carbonate prepared materials.

A. 0.5 at. % Ba sintered at 1100°C for 1 hr.
B. 1.0 at. % Ba sintered at 1100°C for 8 hrs.
C. Undoped packing powder after 32 hrs at 1100°C.

III. DISCUSSION

Great care has been taken during processing raw materials and preparing batches in order to obtain reproducible and reliable data. The extensive experiments carried out to optimize both calcining time and temperature with respect to the fired density were of great value because this method which really optimizes grain size, grain shape, and degree of reaction during calcination provides a starting material with optimal properties for obtaining high density ceramics. Egerton et al.[1] took a step in this direction when he reported that "low-temperature calcines provide good ceramics." The assumption that the optimal calcining conditions determined for materials prepared with carbonates are transferable to materials prepared with nitrates is probably not valid because of the large difference in the decomposition temperatures of these compounds.

Investigations of the sintering behavior of the compound $(Na_{0.5}K_{0.5})NbO_3$ disclosed a great complexity as can be seen from the graphs shown in Figs. 14 through 21.

A. Sintering Mechanisms

Four basic sintering mechanisms for single phase materials by which solid particles in contact may adhere and grow together are given by Kingery and Berg:[12]

1. Volume diffusion
2. Plastic flow
3. Evaporation-condensation
4. Surface diffusion.

However, only volume diffusion and plastic flow result in densification.

Another quite different process which leads to densification is sintering in the presence of a liquid phase. In contrast to the single phase sintering, the densification process in presence of a second phase is markedly accelerated. Kingery[13] and other authors report that (1) an appreciable amount of liquid; (2) an appreciable solubility of the solid in the liquid phase; and (3) a complete wetting of the solid by the liquid are requirements for complete densification.

The main driving force for every sintering mechanism proposed is the decrease of the surface free energy due to the decrease of surface area during densification. Coble's equation for sintering a single phase solid during second and final stage sintering is given as:[14]

$$\frac{dP}{dt} = -\frac{NDγΩ}{l^3kT} \qquad (1)$$

N = geometry factor

D = diffusivity of slowest moving specie

γ = surface energy (solid-vapor)

Ω = vacancy volume

l = grain size

k = Boltzmann's constant

T = temperature

P = porosity

t = time

This equation shows that the sintering rate will decrease by lowering the surface energy.

Assuming a complete wetting of the solid phase in liquid phase sintering and a penetration between grains, the following surface energy relationships are required:

$$\gamma_{sv} > \gamma_{lv} > \gamma_{ss} > 2\gamma_{sl} \qquad (2)$$

where s, l and v refer to solid, liquid and vapor respectively.

In this process with appreciable liquid present or at least sufficient liquid to cover all solid surfaces, the driving force for densification becomes the liquid-vapor surface energy. Even though liquid-vapor surface energies are lower than solid-vapor surface energies, the increase in diffusivity in liquids relative to solids greatly enhances densification rates.

B. Pore Growth

The accelerated densification rate due to the presence of a liquid phase brings the samples to high densities in a very short time where a large portion of the pores can be assumed to be closed. Usually, there will be a negative pressure in each pore given by the relation

$$p = \frac{-2\gamma_{lv}}{r_p} \qquad (3)$$

p = pressure

γ_{lv} = surface energy liquid-vapor

r_p = pore radius

However, if a gas is trapped inside the pores at this state, diffusion of the gas to the surface may become negligible compared with the diffusion flux between the pores and a volume expansion may occur. Gupta and Coble[15] presume that the driving force for densification may approach zero or become negative when the gas trapped inside the pores equilibrates with surface tension and the gas is relatively insoluble in the matrix material. In this case, one or more of the pore growth mechanisms, pore-pore material transfer or pore migration, could become effective. In general, however, a decrease in density implies either a weight loss or a volume expansion or both.

C. Materials Prepared with Carbonates

The relative density of undoped samples sintered for varying times at 1000, 1050 and 1100°C in oxygen atmosphere are given in Fig. 14. The initial densification rate shows a rapid increase with an increase in temperature. This increase may be due to an increasing amount of liquid phase present or a more rapid diffusivity in liquid phase. The curves taken on samples sintered at 1000 and 1050°C show the typical sintering behavior in presence of a liquid phase, whereas the curve taken on samples sintered at a temperature of 1100°C with its very high initial densification rate shows a decrease in density after a transition stage. This de-densification is not accompanied by a weight change of the samples as can be seen from Fig. 19. The constant weight of the samples, even after a sintering time of 8 hrs, indicates an equilibrium situation between the activities of sodium and potassium in sample and packing powder. No material leaves or enters the sample during the de-densification of the undoped sodium-potassium niobate. Thus,

the de-densification has to occur by volume expansion exclusively.

The series of SEM micrographs in Fig. 28 are of undoped samples sintered at 1100°C for varying times; their densities are shown in Fig. 14. Figure 28A shows a sample sintered for 15 min. The microstructure of the fired body shows a relatively uniform grain size with a few large grains interspersed. All grains show a well-developed cubic shape. Figure 28B, taken after a sintering time of 1 hr, shows a very inhomogeneous microstructure with a few grains having a large size of approximately 15 to 20 μm and a large number of much smaller grains having a diameter of 1 to 3 μm. Figure 28C taken on the same material after a sintering time of 4 hrs, reveals that all grains with a diameter less than 5 μm have disappeared leaving a more open structure. A comparison with Fig. 14 shows that this sample already exhibits a large de-densification. Figure 28D shows a sample after a sintering time of 8 hrs. This material exhibits a very open microstructure with large grains and open pores.

These figures imply that the material originating from the small grains is transferred to the large grains which are growing. It is thought that during the growth of the large crystals, their centers are moving apart. This possibility is given by assuming a liquid layer between the cubic grains touching each other as proposed in the model of sintering in presence of a liquid pahse. This assumption is valid because the two phase diagrams, Figs. 1 and 2, indicate a liquid phase in this temperature region (1100°C) if excess Na_2O and K_2O are present. If the initial density is sufficiently high to provide a large portion of closed pores, CO and CO_2 gas originating from a late decomposition

of the carbonates, especially of $BaCO_3$ with its very high decomposition temperature of 1450°C, may equilibrate with the surface tension and stop or reverse the densification.

However, a reverse of densification implies material transfer to the interfaces of touching cubic grains resulting in a moving apart of the grain centers. This behavior of de-densification in the presence of a liquid phase cannot be explained sufficiently by pore-pore material transfer and/or pore migration alone. CO and CO_2 gas which can be assumed to be quite insoluble in the matrix material seem to play an important role in the de-densification of sodium-potassium niobate prepared with carbonates.

Figures 15 through 18 show the relative density of 0.5, 1.0, 2.0 and 4.0 atomic barium doped samples sintered for varying times at 1000, 1050 and 1100°C in an oxygen atmosphere. The initial densification rate undergoes a maximum in the range of 0.5 atomic % dopant indicating a considerable amount of liquid phase present. Furthermore, the de-densification effect seems to have a maximum value in the same region. The weight changes versus linear sintering time for the samples sintered at 1100°C, as given in Fig. 19, indicate a maximum in weight loss for the 0.5 atomic % barium doped material. The curve obtained on material doped with 1.0 atomic % barium shows an initial weight gain followed by a weight loss if the sintering process continues. For this material, weight gain and de-densification coincides. Samples doped with 2.0 atomic % barium and more show a constant weight gain during the sintering process which probably indicates the development of an increased amount of a second phase on the surface of the grains. No de-densification

could be observed in a highly doped material. The initial densification rate drops noticeably with the increasing doping level, Figs. 17 and 18.

Small amounts of barium doped into the material seems to decrease the activities of sodium and potassium in the samples so that the pellets start losing weight, whereas higher amounts of barium lead to an increasing development of a barium-rich second phase on the surface of the grains. This drastic change (see Fig. 19) may be explained by the limited solubility of Ba^{2+} in the solid compound $(Na_{0.5}K_{0.5})NbO_3$. The coincidence of a decreasing initial densification rate with the disappearance of the de-densification effect despite an increasing amount of $BaCO_3$ introduced may indicate that the amount of CO_2 and CO gas are sufficiently high that the gases can leave the sample not allowing large portions of closed pores. The remaining barium may obtain sodium and potassium from the packing powder permeating through these open pores to form the barium-rich second phase. This mechanism would also account for the decreasing initial densification with increasing $BaCO_3$ content and for the steady weight gain even after relatively long sintering times.

The series of SEM micrographs shown in Fig. 26 are taken on samples doped with varying amounts of barium sintered at 1100°C for 8 hrs in oxygen atmosphere. Figures 26A through 26D demonstrate the decrease of grain size by a ratio of approximately 25 to 1 caused by raising the doping level of barium from 0 to 4 atomic %. Figure 26D shows almost no grain growth after a sintering time of 8 hrs in comparison with the powder used for pressing the pellets (Fig. 11A). It is thought that the decrease of grain size is mainly due to the development of the

barium-rich second phase on the surface of the grains.

D. Materials Prepared with Nitrates

Figure 20 shows the relative density of 0.5, 1.0 and 4.0 atomic % barium doped samples sintered for varying times at 1100°C in oxygen atmosphere. The initial sintering rate is noticeably lower than in the materials prepared with carbonates and shows a decrease with increasing amount of dopant. All curves level after a short sintering time and the samples stay at that density. No de-densification effect could be observed. The sintering of these pellets prepared with nitrates and of all pellets prepared with carbonates as well, was conducted in packing powder of the composition $(Na_{0.5}K_{0.5})NbO_3$ having high activities of sodium and potassium.

Further sintering experiments employing the same nitrate prepared materials were carried out using packing powder with excess in Nb_2O_5, i.e., a lower activity in sodium and potassium. These results are given in Fig. 21. The sintering characteristics of these specimens indicate a lower or negligible liquid phase content. Fairly high densities could be obtained with the 0.5 atomic % barium doped material after a sintering time of 15 hrs. No de-densification effects could be observed. Because of the low liquid phase content due to the change in the packing powder composition, it would be possible to raise the sintering temperature and to obtain high densities in shorter times.

Additional sintering experiments using nitrate prepared pellets with high liquid phase contents introduced by adding 5 weight % NaCl showed no densification at all.

The series of pictures shown in Fig. 27 are taken on nitrate prepared samples doped with varying amounts of barium sintered at 1100°C for 8 hrs in oxygen using the packing powder with high activities of sodium and potassium. The decrease in grain size due to the increasing amount of dopant is basically the same as in the carbonate prepared samples, shown in Fig. 26. The decreasing grain size with increasing amount of barium is probably caused by the development of the earlier mentioned barium-rich second phase on the surface of the grains. Investigations made on a representative number of samples employing the electron probe microanalyzer showed a very homogeneous distribution of all elements in the samples. No second phase could be observed but this may be due to the limited resolution of the microprobe, for in some cases, the diameter of the electron beam was greater than the size of the particles investigated.

E. Influence of Barium on the Crystal Structure

The influence of Ba^{2+} on the structure of $(Na_{0.5}K_{0.5})NbO_3$ was determined by means of X-ray diffraction methods. No shift in the Bragg angles (2θ) of the peaks was expected to occur with increasing amounts of barium doped into the material because of the almost identical ionic size of Ba^{2+} and K^{1+}, and no shift could be observed. However, a shift in intensities appeared especially in diffraction peaks containing the "b_o" lattice direction. Figure 22 gives the intensity change observed on the (010) plane. A steady intensity decrease at the (010) line with increasing amount of barium was observed. At 4 atomic % barium the (010) line almost vanishes, which indicates that the unit cell becomes more cubic.

F. Surface Energy and Driving Force for Sintering

All samples examined exhibited a microstructure consisting of cubic grains. The pictures of Fig. 29 show some interesting features of the cubic grains. All cubes have very sharp edges and distinct corners. Intersections of grains are very sharp; no necks can be observed. Figures 28A and 28B show cubes with incomplete layers on their surface. All crystallographic planes appearing in the microstructure of all samples sintered belonged to the cubic {100} family, no other planes could be observed.

It is obvious that this plane must have by far the lowest surface energy of all possible planes. This becomes more clear if one considers the unit cell of $(Na_{0.5}K_{0.5})NbO_3$ in Fig. 24. The {100} planes consist only of the large ions oxygen sodium, and potassium having low ionic potentials. This configuration resembles very much the configuration of the {100} planes in NaCl which are known for their low surface energy. Every other plane in the unit cell of sodium-potassium niobate would expose a niobium (5+) to the surface which would imply a drastic increase of the surface energy. The low surface energy of the (100) planes in contrast with the much higher surface energy of all other possible planes is probably the reason for the absence of any necks in the microstructure and the development of very distinct edges and corners of the cubic grains. Furthermore, this low surface energy of the cubic planes is probably the reason for the reduced sintering rate due to the reduction of the driving force for densification γ as proposed in all sintering models.

IV. SUMMARY

An investigation of the sintering behavior of barium doped and undoped sodium-potassium niobate of the composition $(Na_{0.5}K_{0.5})NbO_3$ has been conducted.

(1) The optimal calcining conditions with respect to the sintered density of $(Na_{0.5}K_{0.5})NbO_3$ prepared with carbonates were found to be 850°C for 2.0 hrs.

(2) A decrease in density for undoped $(Na_{0.5}K_{0.5})NbO_3$ after a sintering time of 2 hrs at a temperature of 1100°C was observed. This de-densification effect was accompanied by a disappearance of all smaller grains in the microstructure and an increase of the pore size.

(3) The de-densification was found to be favored by small amounts of barium doped into the material but inhibited by additions of more than 2 atomic % barium. The de-densification has a maximum in the range of 0.5 atomic % dopant.

(4) It was found that de-densification in undoped sodium-potassium niobate occurs without any detectable weight change of the samples, which implies a negligible amount of material is entering or leaving the pellet during firing. Furthermore, it implies an equilibrium between the activities of all elements in sample and packing powder.

(5) Barium (2+) was found to inhibit grain growth. Even after sintering times of 8 hrs at a temperature of 1100°C the microstructure remained very uniform and the grain size was less than 1 μm.

(6) A slight change in composition of the packing powder from the sodium and potassium-rich side of $(Na_{0.5}K_{0.5})NbO_3$ to the niobium-rich side was found to have a large influence on sintering behavior and

density, by changing the sintering mechanism from liquid phase to solid state sintering.

(7) Indications were found that additions of more than 2.0 atomic % barium lead to a formation of a barium-rich second phase on the surface of the grains. It is possible that this second phase is mainly responsible for the decrease in grain size.

(8) It is postulated that the low surface energy of the {100} planes of $(Na_{0.5}K_{0.5})NbO_3$ formed is the main reason that under conventional sintering the driving force for densification is lowered and densification stops.

ACKNOWLEDGMENTS

The author wishes to thank Professor Richard M. Fulrath under whose guidance this work was carried out.

Appreciation is expressed to Professor Joseph A. Pask, Dr. J. P. Jorgensen, Robert Atkin, Robert Holman and Douglas Lee for their helpful comments and criticism.

I am also grateful to Kelly Radmilovic, George Dahl, Bill Bullis, Jack Wodei, and George Georgakopoulos for their experimental assistance. Finally, I am especially indebted to my wife, Uta, for her encouragements.

This work was carried out under the auspices of the United States Atomic Energy Commission.

REFERENCES

1. L. Egerton and D. M. Dillon, "Piezoelectric and Dielectric Properties of Ceramics in the System Potassium-Sodium Niobate," J. Am. Ceram. Soc., 42 [9] pp. 438-442 (1959).

2. J. E. May, Jr., "Ultrasonic Delay Lines," Bell Labs. Record 35 [1], pp. 212-216 (1956).

3. G. Shirane, B. Newnham, and R. Pepinsky, "Dielectric Properties and Phase Transitions of $NaNbO_3$ and (Na, K)NbO_3," Phys. Rev. 96 [3] pp. 581-588 (1954).

4. R. H. Dungan and R. D. Golding, "Polarization of $NaNbO_3$-$KNbO_3$ Solid Solutions," J. Am. Ceram. Soc. 48 [11] p. 601 (1965).

5. R. E. Jaeger and L. Egerton, "Hot Pressing of Potassium-Sodium Niobates," J. Am. Ceram. Soc. 45 [5] pp. 209-213 (1962).

6. L. Egerton and C. A. Bieling, "Isostatically Hot-Pressed Sodium-Potassium Niobate Transducer Material for Ultrasonic Devices," Am. Ceram. Soc. Bull. 47 [12] pp. 1151-1156 (1968).

7. A. Reisman and F. Holtzberg, "Phase Equilibria in the System K_2CO_3-Nb_2O_5 by the Method of Differential Thermal Analysis," J. Am. Chem. Soc. 77, p. 2115 (1955).

8. M. W. Shafer and Rustum Roy, "Phase Equilibrium in the System Na_2O-Nb_2O_5," J. Am. Ceram. Soc. 42 [10], pp. 482-486 (1959).

9. A. Reisman, F. Holtzberg and E. Banks, "Relations of the Group VB Pentoxides with Alkali Oxides and Carbonates. VII. Heterogeneous Equilibria in the System Na_2O or Na_2CO_3-Nb_2O_5," J. Am. Chem. Soc. 80, p. 37 (1958).

10. D. Burnett, D. Clinton and R. P. Miller, "Some Phase Relationships Within the System Na_2O-B_2O_3-Nb_2O_5," J. Mat. Sci. 3 pp. 47-60 (1968).

11. L. V. Azaroff, "Elements of X-ray Crystallography," New York, 1968, McGraw-Hill.

12. W. D. Kingery and M. Berg, "Study of the Initial Stages of Sintering Solids by Viscous Flow, Evaporation-Condensation and Self-Diffusion," J. Appl. Phys., 26 (10) 1205 (1955).

13. W. D. Kingery, "Densification During Sintering in the Presence of a Liquid Phase. I. Theory," J. Appl. Phys. 30 (3) 301 (1958).

14. R. L. Coble, "Sintering Crystalline Solids. I. Intermediate and Final Stage Diffusion Models," J. Appl. Phy. 32 (5) 787 (1961).

15. T. K. Gupta and R. L. Coble, "Sintering of ZnO: II, Density Decrease and Pore Growth During the Final Stage of the Pores," J. Am. Ceram. Soc. 51 [9] pp. 525-528 (1968).

LEGAL NOTICE

This report was prepared as an account of Government sponsored work. Neither the United States, nor the Commission, nor any person acting on behalf of the Commission:

A. Makes any warranty or representation, expressed or implied, with respect to the accuracy, completeness, or usefulness of the information contained in this report, or that the use of any information, apparatus, method, or process disclosed in this report may not infringe privately owned rights; or

B. Assumes any liabilities with respect to the use of, or for damages resulting from the use of any information, apparatus, method, or process disclosed in this report.

As used in the above, "person acting on behalf of the Commission" includes any employee or contractor of the Commission, or employee of such contractor, to the extent that such employee or contractor of the Commission, or employee of such contractor prepares, disseminates, or provides access to, any information pursuant to his employment or contract with the Commission, or his employment with such contractor.

TECHNICAL INFORMATION DIVISION
LAWRENCE RADIATION LABORATORY
UNIVERSITY OF CALIFORNIA
BERKELEY, CALIFORNIA 94720